
GAIN: ENHANCING BYZANTINE ROBUSTNESS IN FEDERATED LEARNING WITH GRADIENT DECOMPOSITION

Yuchen Liu
Zhejiang University

Chen Chen
Sony AI

Lingjuan Lyu
Sony AI

Fangzhao Wu
Microsoft

Sai Wu
Zhejiang University

Gang Chen
Zhejiang University

ABSTRACT

Federated learning provides a privacy-aware learning framework by enabling participants to jointly train models without exposing their private data. However, federated learning has exhibited vulnerabilities to Byzantine attacks, where the adversary aims to destroy the convergence and performance of the global model. Meanwhile, we observe that most existing robust AGgregation Rules (AGRs) fail to stop the aggregated gradient deviating from the optimal gradient (the average of honest gradients) in the non-IID setting. We attribute the reason of the failure of these AGRs to two newly proposed concepts: identification failure and integrity failure. The identification failure mainly comes from the exacerbated curse of dimensionality in the non-IID setting. The integrity failure is a combined result of conservative filtering strategy and gradient heterogeneity. In order to address both failures, we propose GAIN, a gradient decomposition scheme that can help adapt existing robust algorithms to heterogeneous datasets. We also provide convergence analysis for integrating existing robust AGRs into GAIN. Experiments on various real-world datasets verify the efficacy of our proposed GAIN.

1 Introduction

Federated Learning (FL) [1] is a privacy-aware distributed machine learning paradigm. It has recently attracted widespread attention as a result of emerging data silos and growing privacy awareness [2, 3]. In this paradigm, data owners (clients) repeatedly use their private data to compute local gradients and send them to a central server for aggregation. In this way, clients can collaborate to train a model without exposing their private data. However, the distributed property of FL also makes it vulnerable to Byzantine attacks [4, 5, 6, 7]. During the training phase, Byzantine clients can send arbitrary messages to the central server to bias the global model. Moreover, it is challenging for the central server to identify the Byzantine clients, since the server can neither access clients' training data nor monitor local training processes.

In order to defend against Byzantine attacks, the community has proposed a wealth of defenses [4, 5, 8]. Most defenses abandon the averaging step adopted by conventional FL frameworks, e.g., FedAvg [1]. Instead, they use robust AGgregation Rules (AGRs) to aggregate local gradients in order to defend against Byzantine attacks. Most existing robust AGRs assume that the data distribution on different clients is identically and independently distributed (IID) [9, 10]. However, the data is usually non-independent and identically distributed (non-IID) in real-world FL applications [1, 11, 12]. As a result, in more realistic non-IID settings, most robust AGRs fail to defend against Byzantine attacks, and thus suffer from significant performance degradation [13, 14].

To investigate the cause of the degradation, we perform a thorough experimental study on various robust AGRs. Close inspection reveals that the reason behind the degradation is different for different AGRs with different types of aggregation strategies. For *conservative* AGRs that only aggregate few gradients to get rid of Byzantines, they suffer from *integrity* failure. The integrity failure describes that an AGR can only identify *few* honest gradients for aggregation. This failure will lead to an aggregated gradient with limited utility due to the gradient heterogeneity [15, 11] in the non-IID setting. For *radical* AGRs that aggregate as many gradients as possible to avoid such deviation, they suffer from another *identification* failure. The identification failure means that an AGR fails to distinguish between honest and

Byzantine gradients. This failure is mainly due to the curse of dimensionality [5, 16] aggravated by the non-IIDness. Both failures deviate the aggregated gradient from the optimal gradient (the average of honest gradients). As a result, most existing AGRs fail to achieve a satisfactory performance in the non-IID setting.

Motivated by the above observations, we propose a GrAdient decomposItion method called GAIN that can handle both failures in various non-IID settings. In particular, to address the identification failure due to the curse of dimensionality, GAIN decomposes each high-dimensional gradient into low-dimensional groups for gradient identification. Then, GAIN incorporates gradients with low identification scores into final aggregation to tackle the integrity failure.

Our contributions in this work are summarized below.

- We reveal the root reasons for the performance degradation of current robust AGRs in the non-IID setting by proposing two new concepts: integrity failure and identification failure. Integrity failure originates from the gradient heterogeneity, and identification failure is a result of the aggravated curse of dimensionality in the non-IID setting.
- We propose a novel and compatible approach called GAIN, which applies robust AGRs on the decomposed gradients, followed by identification before aggregation, rather than directly operating on the original gradients as the existing defenses (Multi-Krum [4], Bulyan [5], etc) do.
- We also provide convergence analysis for integrating existing robust AGRs into GAIN. In particular, we provide an upper bound for the sum of gradient norms.
- We also offer empirical experiments on three real-world datasets across various settings to validate the effectiveness and superiority of our GAIN.

2 Related Works

Byzantine robust learning is first introduced by [4]. Subsequently, a range of works study the robustness against Byzantine attacks by proposing various robust AGgregation Rules (AGR) under the IID setting. Generally, we can classify the current robust AGRs into two categories: **conservative** AGRs and **radical** AGRs.

Typical conservative AGRs, including Bulyan [5], Median [8], Trimmed Mean [8], etc., only aggregate few gradients to reduce the risk of the introduced Byzantine gradients. Bulyan [5] applies a variant of trimmed mean as a post-processing method to handle the curse of dimensionality. [8] theoretically analyze the statistical optimality of Median and Trimmed Mean. The radical AGRs, e.g., Multi-Krum [4], DnC [17], incorporate as many gradients as possible to avoid such deviation. Multi-Krum is a distance-based AGR proposed by [4]. [18] discuss the Byzantine robustness of Geometric Median and propose a computationally efficient approximation. [17] propose to perform dimensionality reduction using random sampling, followed by spectral-based outlier removal. Recently, a quantity of works [19, 20, 21, 22] discuss the effect of distributed momentum to Byzantine robustness from different perspectives. However, in more realistic FL applications where the data is non-IID, the efficacy of these defenses are quite limited. They fail to obtain high-quality aggregated gradient in the non-IID setting, thus suffer from significant performance degradation.

Recently works have also explored defenses that can be applicable to the non-IID setting. [23] can only achieve Byzantine robustness when the server has a validation set, which compromises the privacy principle of the FL [1]. [24] adapt a robust mean estimation algorithm to FL to combat Byzantines in the non-IID setting. However, it requires $\Omega(d^2)$ time (d is the number of model parameters), which is unacceptable due to the high dimensionality of model parameters. [25] consider Byzantine robustness in the asynchronous communication and unconstrained topologies settings. [14] propose to apply geometric median only to the sparsified gradients to save computation cost. [13] perform a bucketing process before aggregation to reduce the gradient heterogeneity. These methods guarantee convergence of SGD in the existence of Byzantines. However, convergence is not enough in the context of non-convex, high dimensional case of neural networks [5]. These methods lack of the guarantee that the aggregated gradient does not deviate from the optimal gradient (the average of honest gradients). As a result, they may lead to convergence towards ineffectual models.

3 Notations and Preliminaries

Notations. For any positive integer $n \in \mathbb{N}^+$, we denote the set $\{1, \dots, n\}$ by $[n]$. The cardinality of a set S is denoted by $\#S$ or $|S|$. For a real number $x \in \mathbb{R}$, we use $|x|$ to denote the absolute value of number x . We denote the ℓ_2 norm of vector \mathbf{x} by $\|\mathbf{x}\|$. We use $[\mathbf{x}]_j$ to represent the j -th component of vector \mathbf{x} . The sub-vector of vector \mathbf{x} indexed by index set \mathcal{J} is denoted by $[\mathbf{x}]_{\mathcal{J}} = ([\mathbf{x}]_{j_1}, \dots, [\mathbf{x}]_{j_k})$, where $\mathcal{J} = \{j_1, \dots, j_k\}$, and $k = |\mathcal{J}|$ is the number of indices. For a random variable X , we use $\mathbb{E}[X]$ and $\text{Var}[X]$ to denote the expectation and variance of X , respectively.

Federated learning. We consider the federated learning system with a center server and n clients following [4, 8, 5]. Then the objective is to minimize loss $\mathcal{L}(\mathbf{w})$ defined as follows.

$$\mathcal{L}(\mathbf{w}) = \frac{1}{n} \sum_{i=1}^n \mathcal{L}_i(\mathbf{w}), \quad \text{where } \mathcal{L}_i(\mathbf{w}) = \mathbb{E}_{\xi_i}[\mathcal{L}(\mathbf{w}; \xi_i)], i \in [n], \quad (1)$$

where \mathbf{w} is the model parameter, \mathcal{L}_i is the loss function on the i -th client, ξ_i is the data distribution on the i -th client, and $\mathcal{L}(\mathbf{w}; \xi)$ is the loss function.

In the t -th communication round, the server distributes the parameter \mathbf{w}^t to the clients. Each client i conducts several epochs of local training on local data to obtain the updated local parameter \mathbf{w}_i^t . Then, client i computes the local gradient \mathbf{g}_i^t as follows and sends it to the server.

$$\mathbf{g}_i^t = \mathbf{w}^t - \mathbf{w}_i^t. \quad (2)$$

Finally, the server collects the local gradients and uses the average gradient to update the global model.

$$\mathbf{w}^{t+1} = \mathbf{w}^t - \mathbf{g}^t, \quad \mathbf{g}^t = \frac{1}{n} \sum_{i=1}^n \mathbf{g}_i^t. \quad (3)$$

This process is repeated until the global model converges or the number of communication rounds reaches the set value T .

Byzantine threat model. In real-world applications, not all clients in FL systems are honest. In other words, there may exist Byzantine clients in FL systems [4]. Suppose that an adversary controls f Byzantine clients among the total n clients. Let $\mathcal{B} \in [n]$ denote set of Byzantine clients and $\mathcal{H} = [n] \setminus \mathcal{B}$ denote the set of honest clients. In the presence of Byzantine clients, the uploaded message of client i in the t -th communication round is

$$\mathbf{g}_i^t = \begin{cases} \mathbf{w}_i^{t+1} - \mathbf{w}^t, & i \in \mathcal{H}, \\ *, & i \in \mathcal{B}, \end{cases} \quad (4)$$

where $*$ represents arbitrary value.

Robust AGRs. Most solutions replace the averaging step by a robust alternative to defend against Byzantine attacks. More specifically, the server aggregates the gradients and updates the global model as follows.

$$\mathbf{w}^{t+1} = \mathbf{w}^t - \hat{\mathbf{g}}^t, \quad \hat{\mathbf{g}}^t = \mathcal{A}(\mathbf{g}_1^t, \dots, \mathbf{g}_n^t), \quad (5)$$

where $\hat{\mathbf{g}}^t$ is the aggregated gradient, and \mathcal{A} is a robust AGR, e.g., Multi-Krum [4], Bulyan [5].

For notation simplicity, we omit the superscript t of the gradient symbols when there is no ambiguity in the rest of this paper.

4 Failures of existing Robust AGRs in the Non-IID Setting

Most robust AGRs focus on Byzantine robustness in the IID setting [4, 5]. When the data is non-IID, the performance of these robust AGRs drop drastically [17, 13]. In order to understand the root cause of this performance drop, we perform an experimental study on various robust AGRs. Particularly, we examine the behaviors of robust AGRs under the attack of 20% Byzantines in both IID and non-IID settings on CIFAR-10 [26] in Figure 1. More detailed setups are covered in Appendix A. A close inspection reveals that AGRs of different types demonstrate different failures in the non-IID setting. As mentioned earlier in Sec. 2, most robust AGRs fall under the umbrella of either *conservative* AGRs or *radical* AGRs. Next, we choose two representative AGRs (Bulyan and Multi-Krum) from both types and summarize how they fail in the non-IID setting.

Integrity failure of a conservative AGR. We take a closer look at a representative conservative AGR – Bulyan [5]. Specifically, we consider an indicator called *honest ratio* – the ratio of selected honest client number to all selected client number (# selected honest clients / # selected clients) of a robust AGR in each communication round. A higher honest ratio suggests a higher proportion of honest gradients among the gradients aggregated by AGR. In particular, honest ratio 1 (0) suggests that all gradients that the AGR aggregates are honest (Byzantine). In Figure 1(a), we report the honest ratio of the conservative AGR (Bulyan) in both IID and non-IID settings. The results show that in both settings, all the gradients aggregated by the conservative AGR are honest, which demonstrates the strong Byzantine filtering ability of a conservative AGR. Unfortunately, we find that Byzantine filtering is not enough in the non-IID setting. The results in Figure 1(b) illustrate that the accuracy is significantly lower in the non-IID setting. This performance

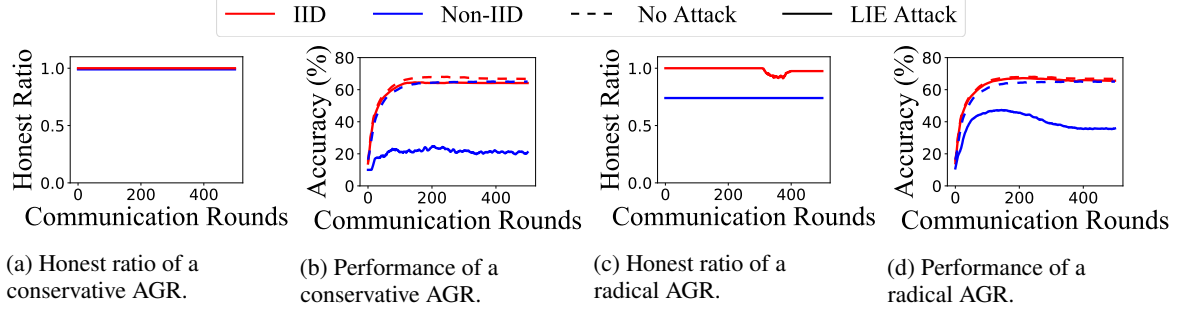


Figure 1: The behaviors of a conservative AGR (Bulyan) and a radical AGR (Multi-Krum) under the attack of 20% Byzantines in both IID and non-IID settings on CIFAR-10 dataset. More detailed setups are covered in Appendix A. The dotted lines represent the performance without Byzantines.

degradation implies a sharp deviation of the aggregated gradient from the *optimal* gradient (the average of honest gradients) in the non-IID setting. Honest gradients are heterogeneous when the data is non-IID [15, 27, 11]. As a result, aggregating only partial honest gradients will deviate the aggregated gradient from the optimal gradient, and eventually lead to ineffectual models. Therefore, in addition to Byzantine filtering, *it is also crucial to incorporate sufficient honest gradients into aggregation in the non-IID setting.*

Identification failure of a radical AGR. We closely examine a typical radical AGR – Multi-Krum [4]. In Figure 1(c), we demonstrate the honest ratio of the radical AGR in both IID and non-IID settings. As shown in the figure, the radical AGR succeeds in identifying honest gradients for aggregation in the IID setting but fails in the non-IID setting. The critical reason behind is that while the curse of dimensionality [5] can be provably addressed in the IID setting, it will be aggravated and intractable in the non-IID setting. When the data is non-IID, Byzantines can easily exploit the curse of dimensionality to compromise radical AGRs, thus degrade the utility of global model as shown in Figure 1(d). Therefore, *it is critical to overcome the aggravated curse of dimensionality in the non-IID setting.*

As analyzed above, most robust AGRs suffer from identification failure and integrity failure due to gradient heterogeneity and the aggravated curse of dimensionality in the non-IID setting. As a result, they fail to stop the aggregated gradient deviating from the optimal gradient, which leads to unsatisfactory performance in the non-IID setting.

5 Proposed Method

Our observations in Sec. 4 clearly motivate the need for a more robust defense to defeat Byzantine attacks in the non-IID setting. Inspired by these observations, we propose a novel GrAdient decomposItion method called GAIN, which consists of three stages as follows.

Decomposition. First, GAIN decomposes the gradients for gradient identification. The decomposition is specified by a partition of set $[d]$, where d is the dimension of gradients. Let $\{\mathcal{J}_1, \dots, \mathcal{J}_p\}$ denote the partition, where p is the number of groups. Particularly, the partition satisfies:

$$\mathcal{J}_q \neq \emptyset, \quad \forall q \in [p] \quad \text{and} \quad [d] = \bigcup_{q=1}^p \mathcal{J}_q, \quad \text{and} \quad \mathcal{J}_q \cap \mathcal{J}_{q'} = \emptyset, \quad \forall q, q' \in [p], q \neq q', \quad (6)$$

where \emptyset represents the empty set, \bigcup represents the union of sets, and \bigcap represents the intersection of sets. Each gradient \mathbf{g}_i is correspondingly decomposed into p sub-vectors as follows.

$$\mathbf{g}_i^{(q)} = [\mathbf{g}_i]_{\mathcal{J}_q}, \quad i \in [n], q \in [p], \quad (7)$$

where $\mathbf{g}_i^{(q)}$ is the q -th sub-vector of gradient \mathbf{g}_i .

Identification. Then, GAIN applies any robust AGR \mathcal{A} to each group of sub-vectors corresponding to \mathcal{J}_q :

$$\hat{\mathbf{g}}^{(q)} = \mathcal{A}(\mathbf{g}_1^{(q)}, \dots, \mathbf{g}_n^{(q)}), \quad q \in [p], \quad (8)$$

where $\hat{\mathbf{g}}^{(q)}$ is the aggregation result of group q . By performing aggregation on groups of low-dimensional sub-vectors, GAIN can circumvent the curse of dimensionality, thus avoiding the identification failure discussed in Sec. 4. In other words, $\hat{\mathbf{g}}^{(q)}$ can get rid of Byzantines.

Note that $\hat{\mathbf{g}}^{(q)}$ may still suffer from deviation due to the integrity failure of the AGR \mathcal{A} as illustrated in Sec. 4. Therefore, it is inappropriate to directly use the aggregation results $\{\hat{\mathbf{g}}^{(q)}, q \in [p]\}$ as the final output. Instead, we use $\hat{\mathbf{g}}^{(q)}$ as an honest reference to compute identification scores for each client as follows.

$$s_i^{(q)} = \|\mathbf{g}_i^{(q)} - \hat{\mathbf{g}}^{(q)}\|, \quad i \in [n], q \in [p]. \quad (9)$$

Since the group-wise aggregation result $\hat{\mathbf{g}}^{(q)}$ can get rid of Byzantines, the identification score $s_i^{(q)}$ can provably characterize the potential for the $\mathbf{g}_i^{(q)}$ being a sub-vector of an honest gradient. Then, GAIN collects the identification scores from all groups and computes the final aggregation result. In particular, the final identification score s_i of each client is composed of its identification scores received from all groups as follows.

$$s_i = \sum_{q=1}^p s_i^{(q)}, \quad i \in [n]. \quad (10)$$

Aggregation. To avoid integrity failure, GAIN selects total $n - f$ gradients with the lowest identification scores for aggregation. Let \mathcal{I} denote the index set of selected gradients, then the average of selected gradients is output as the final aggregation result as follows:

$$\hat{\mathbf{g}} = \frac{1}{n - f} \sum_{i \in \mathcal{I}} \mathbf{g}_i. \quad (11)$$

Note that in the first stage (Decomposition) of GAIN, \mathcal{A} could be any c -resilient AGR (Definition 1). The key difference lies in that all the existing robust AGRs (Multi-Krum, Bulyan, etc) directly operate on the original gradients before aggregation; instead we propose to apply robust AGRs on the decomposed gradient, followed by identification before aggregation. In this way, we can help enhance the identification ability and integrity of the current robust AGRs that satisfy the c -resilient property (Definition 1) in the non-IID setting. Detailed theoretical analysis and empirical support can be referred to Sec. 6 and Sec. 7 respectively.

6 Theoretical Analysis

In this section, we provide a convergence analysis for our GAIN approach.

We analyze a popular FL model widely considered by [20, 13, 14]. In particular, each local gradient is computed by SGD as follows.

$$\mathbf{g}_i^t = \nabla \mathcal{L}(\mathbf{w}^t; \boldsymbol{\xi}_i^t), \quad i \in [n], \quad (12)$$

where $\boldsymbol{\xi}_i^t$ represents a minibatch uniformly sampled from the local data distribution $\boldsymbol{\xi}_i$ in the t -th communication round, and $\nabla \mathcal{L}(\mathbf{w}^t, \boldsymbol{\xi}_i^t)$ represents the gradient of loss over the minibatch $\boldsymbol{\xi}_i^t$.

We make the following assumptions, which are standard in FL [20, 13, 14].

[Unbiased Estimator] The stochastic gradients sampled from any local data distribution are unbiased estimators of local gradients over \mathbb{R}^d for all clients, i.e.,

$$\begin{aligned} \mathbb{E}_{\boldsymbol{\xi}_i^t} [\nabla \mathcal{L}_i(\mathbf{w}; \boldsymbol{\xi}_i^t)] &= \nabla \mathcal{L}_i(\mathbf{w}), \\ \forall \mathbf{w} \in \mathbb{R}^d, i \in [n], t \in \mathbb{N}^+. \end{aligned} \quad (13)$$

[Bounded Variance] The variance of stochastic gradients sampled from any local data distribution is uniformly bounded over \mathbb{R}^d for all clients, i.e., there exists $\sigma \geq 0$ such that

$$\begin{aligned} \mathbb{E} \|\nabla \mathcal{L}_i(\mathbf{w}; \boldsymbol{\xi}_i^t) - \nabla \mathcal{L}_i(\mathbf{w})\|^2 &\leq \sigma^2, \\ \forall \mathbf{w} \in \mathbb{R}^d, i \in [n], t \in \mathbb{N}^+. \end{aligned} \quad (14)$$

[Gradient Dissimilarity] The difference between the local gradients and the global gradient is uniformly bounded over \mathbb{R}^d for all clients, i.e., there exists $\kappa \geq 0$ such that

$$\|\nabla \mathcal{L}_i(\mathbf{w}) - \nabla \mathcal{L}(\mathbf{w})\|^2 \leq \kappa^2, \quad \forall \mathbf{w} \in \mathbb{R}^d, i \in [n]. \quad (15)$$

We consider arbitrary non-convex loss function $\mathcal{L}(\cdot)$ that satisfies the following Lipschitz condition. This condition is widely applied in the convergence analysis of Byzantine-robust federated learning [13, 19, 25]. [Lipschitz Smoothness] The loss function is L -Lipschitz smooth with respect over \mathbb{R}^d , i.e.,

$$\begin{aligned} \|\nabla \mathcal{L}(\mathbf{w}) - \nabla \mathcal{L}(\mathbf{w}')\| &\leq L\|\mathbf{w} - \mathbf{w}'\|, \\ \forall \mathbf{w}, \mathbf{w}' &\in \mathbb{R}^d. \end{aligned} \quad (16)$$

Sec. 6 establishes the unbiased property of stochastic gradient. Sec. 6 bounds the variance of the stochastic gradients within a client. And Sec. 6 is a common measure of the non-IID level in federated learning [24, 11, 13].

We consider robust AGRs that satisfy the following robustness criterion (Definition 1) introduced by [28]. A wide class of state-of-the-art AGRs satisfy this criterion [28].

Definition 1 ((f, λ) -resilient). *For $f \leq n$ and real value λ , an AGR \mathcal{A} is called (f, λ) -resilient if for any input $\{\mathbf{x}_1, \dots, \mathbf{x}_n\}$ and any set $\mathcal{S} \subseteq [n]$ of size $n - f$, the output of \mathcal{A} satisfies:*

$$\|\mathcal{A}(\mathbf{x}_1, \dots, \mathbf{x}_n) - \bar{\mathbf{x}}_{\mathcal{S}}\| \leq \lambda \max_{i, i' \in \mathcal{S}} \|\mathbf{x}_i - \mathbf{x}_{i'}\|, \quad (17)$$

where $\bar{\mathbf{x}}_{\mathcal{S}} = \sum_{i \in \mathcal{S}} \mathbf{x}_i / |\mathcal{S}|$.

We show that given any (f, λ) -resilient base AGR \mathcal{A} , our GAIN can help the global model to reach a better parameter point.

Suppose Sec. 6 hold, and let $\eta = 1/2L$. Given an (f, λ) -resilient robust AGR \mathcal{A} , we start from \mathbf{w}^0 and run GAIN for T communication rounds, it satisfies

$$\mathcal{L}(\mathbf{w}^0) \geq \frac{3}{16L} \sum_{t=1}^T (\|\nabla \mathcal{L}(\mathbf{w}^t)\|^2 - e^2), \quad (18)$$

where

$$e^2 = \mathcal{O}((\kappa^2 + \sigma^2)(1 + \frac{n-f+1}{p})(1 + c^2 + \frac{1}{n-f})\frac{f^2}{(n-f)^2}). \quad (19)$$

Please refer to Appendix B.1 for the proof. Sec. 6 provides an upper bound for the sum of gradient norms in presence of Byzantine gradients. Equation (18) indicates that as the number of communication rounds increases, we can find an approximate optimal parameter \mathbf{w} with $\|\nabla \mathcal{L}(\mathbf{w})\| \leq e$. Furthermore, as the number of sub-vectors p increases, the approximation becomes better, i.e., e^2 decreases, which validates the efficacy of our approach. From another aspect, Sec. 6 also characterizes the fundamental difficulties of Byzantine-robust federated learning in the non-IID setting. The negative term $-e^2$ on the RHS implies that FL may never converge to an optimal point. By contrast, the global model may wander among sub-optimal points. What's more, even after reaching the convergence point, the global model may step into another sub-optimal in the next communication round. A detailed comparison of the convergence results between our approach and recent works is presented in Appendix B.2.

7 Experiments

7.1 Experimental Setups

Datasets. Our experiments are conducted on three real-world datasets: CIFAR-10 [26], CIFAR-100 [26], a subset of ImageNet [29] referred as ImageNet-12 and FEMNIST [30]. CIFAR-10 dataset consists of 60,000 32×32 color images in 10 classes, with 6,000 images per class. There are 50,000 training images and 10,000 test images in CIFAR-10 dataset. CIFAR-100 dataset consists of 60,000 32×32 color images in 100 classes, with 600 images per class. There are 50,000 training images and 10,000 test images in CIFAR-100 dataset. ImageNet-12 consists of 15,600 color images in 12 classes, with 1,300 images per class. There are 12,480 training images and 3,120 test images in this subset of ImageNet. FEMNIST consists of 817,851 28×28 gray-scale images in 62 classes. There are 772,066 training images and 857,85 test images in FEMNIST.

For FEMNIST, the data is naturally partitioned into 3,597 clients based on the writer of the digit/character. For each client, we randomly sample a 0.9 portion of data as the training data and let the remaining 0.1 portion of data be the test data following [30]. Intuitively, the data distribution across different clients is non-IID.

Table 1: Accuracy (mean \pm std) of different defenses under 6 attacks on CIFAR-10, ImageNet-12, FEMNIST, and CIFAR-100.

Dataset	Attack	BitFlip	LabelFlip	LIE	Min-Max	Min-Sum	IPM
CIFAR-10	Multi-Krum	43.19 \pm 0.38	43.90 \pm 0.03	37.03 \pm 1.62	39.06 \pm 0.07	23.68 \pm 0.18	36.47 \pm 0.22
	GAIN (Multi-Krum)	59.23 \pm 0.55	61.47 \pm 0.26	55.66 \pm 0.93	49.19 \pm 0.72	53.59 \pm 0.96	56.94 \pm 3.60
	Bulyan	54.10 \pm 0.19	55.12 \pm 0.14	30.58 \pm 0.75	29.03 \pm 1.10	46.19 \pm 0.92	33.88 \pm 0.61
	GAIN (Bulyan)	59.14 \pm 0.01	61.21 \pm 0.60	48.90 \pm 0.83	48.35 \pm 1.58	53.74 \pm 0.71	56.53 \pm 1.51
	Median	45.41 \pm 0.44	51.88 \pm 0.62	28.75 \pm 0.35	32.72 \pm 0.81	37.39 \pm 0.90	43.21 \pm 0.47
	GAIN (Median)	59.28 \pm 0.24	61.24 \pm 1.34	46.60 \pm 0.13	49.37 \pm 1.13	53.32 \pm 1.90	56.33 \pm 0.82
	RFA	49.61 \pm 0.31	44.35 \pm 0.31	15.39 \pm 0.37	16.62 \pm 0.83	18.22 \pm 0.43	45.92 \pm 0.13
	GAIN (RFA)	53.35 \pm 0.30	62.25 \pm 0.56	52.69 \pm 0.89	52.64 \pm 1.48	56.16 \pm 0.91	62.26 \pm 1.27
CIFAR-100	DnC	58.63 \pm 1.29	60.82 \pm 1.56	61.07 \pm 0.72	60.42 \pm 0.59	53.71 \pm 0.96	59.99 \pm 0.82
	GAIN (DnC)	58.96 \pm 0.60	61.02 \pm 0.27	61.87 \pm 0.51	61.04 \pm 1.18	54.36 \pm 1.12	57.92 \pm 1.71
	RBTM	54.27 \pm 1.63	59.60 \pm 1.76	47.67 \pm 2.51	49.02 \pm 0.31	50.74 \pm 0.06	55.27 \pm 1.60
	GAIN (RBTM)	59.41 \pm 0.20	60.75 \pm 0.19	52.10 \pm 1.28	49.60 \pm 0.17	53.63 \pm 0.58	56.65 \pm 1.52
	Multi-Krum	34.27 \pm 0.28	35.57 \pm 0.94	17.17 \pm 0.08	16.77 \pm 0.78	22.89 \pm 0.61	15.93 \pm 2.00
	GAIN (Multi-Krum)	42.41 \pm 0.58	42.55 \pm 0.12	27.81 \pm 0.32	31.18 \pm 1.48	41.33 \pm 0.50	42.62 \pm 1.53
	Bulyan	35.77 \pm 0.18	42.60 \pm 0.07	35.41 \pm 0.40	35.53 \pm 1.38	39.13 \pm 0.12	40.27 \pm 1.64
	GAIN (Bulyan)	42.28 \pm 1.61	43.77 \pm 0.46	38.39 \pm 0.19	36.33 \pm 1.51	40.73 \pm 0.39	42.88 \pm 0.14
FEMNIST	Median	36.62 \pm 0.12	41.64 \pm 0.76	22.75 \pm 0.04	23.21 \pm 0.71	30.68 \pm 0.26	40.98 \pm 0.38
	GAIN (Median)	42.41 \pm 0.66	42.62 \pm 0.09	35.16 \pm 1.08	36.46 \pm 0.10	41.08 \pm 0.04	43.63 \pm 2.85
	RFA	21.32 \pm 0.84	28.76 \pm 1.33	25.63 \pm 0.20	26.46 \pm 1.83	28.33 \pm 0.93	21.36 \pm 0.54
	GAIN (RFA)	42.64 \pm 0.44	42.42 \pm 0.25	26.30 \pm 1.08	30.30 \pm 0.12	41.09 \pm 0.66	43.45 \pm 0.52
	DnC	41.77 \pm 0.62	42.93 \pm 0.07	42.95 \pm 1.03	40.15 \pm 0.70	40.02 \pm 1.07	41.23 \pm 2.29
	GAIN (DnC)	43.35 \pm 0.41	43.57 \pm 1.11	43.64 \pm 0.11	41.66 \pm 0.78	41.02 \pm 1.39	43.25 \pm 0.43
	RBTM	36.35 \pm 0.17	42.67 \pm 1.55	24.06 \pm 0.09	26.24 \pm 1.04	36.51 \pm 0.40	43.12 \pm 1.12
	GAIN (RBTM)	43.44 \pm 0.81	43.19 \pm 2.65	33.14 \pm 0.58	34.35 \pm 0.76	41.51 \pm 0.93	43.20 \pm 0.76
ImageNet-12	Multi-Krum	67.65 \pm 0.23	57.43 \pm 1.25	44.58 \pm 0.07	28.32 \pm 0.31	29.98 \pm 0.45	12.26 \pm 1.34
	GAIN (Multi-Krum)	84.29 \pm 1.76	85.45 \pm 0.40	74.76 \pm 1.74	57.46 \pm 0.33	70.65 \pm 1.35	81.46 \pm 0.18
	Bulyan	77.58 \pm 1.30	79.39 \pm 2.14	56.43 \pm 0.45	35.10 \pm 0.69	44.83 \pm 1.40	5.91 \pm 0.17
	GAIN (Bulyan)	84.90 \pm 0.69	83.68 \pm 0.76	71.43 \pm 1.07	66.22 \pm 0.47	71.76 \pm 0.99	82.97 \pm 1.04
	Median	80.25 \pm 0.06	76.86 \pm 1.96	64.88 \pm 0.23	50.67 \pm 0.37	61.33 \pm 0.13	71.98 \pm 0.77
	GAIN (Median)	84.59 \pm 0.14	85.67 \pm 0.48	76.19 \pm 0.43	65.84 \pm 0.41	70.84 \pm 0.86	82.18 \pm 0.40
	RFA	5.46 \pm 0.06	5.46 \pm 0.01	5.46 \pm 0.05	5.46 \pm 0.03	5.46 \pm 0.02	5.59 \pm 0.09
	GAIN (RFA)	84.86 \pm 0.78	84.59 \pm 0.20	69.82 \pm 0.33	69.18 \pm 0.09	77.67 \pm 1.31	86.08 \pm 2.51
ImageNet-12	DnC	8.90 \pm 0.31	77.71 \pm 0.03	78.52 \pm 0.28	8.29 \pm 0.37	74.18 \pm 0.03	74.70 \pm 1.57
	GAIN (DnC)	84.71 \pm 0.39	85.39 \pm 0.64	82.54 \pm 0.26	74.37 \pm 0.50	75.41 \pm 0.22	82.73 \pm 1.22
	RBTM	82.57 \pm 0.34	81.57 \pm 1.12	59.93 \pm 0.20	65.20 \pm 0.60	71.82 \pm 0.73	76.88 \pm 1.75
	GAIN (RBTM)	84.89 \pm 1.94	85.44 \pm 0.20	73.38 \pm 0.31	66.24 \pm 0.94	75.50 \pm 1.13	82.58 \pm 1.85
	Multi-Krum	44.36 \pm 1.52	34.04 \pm 1.69	45.38 \pm 1.04	48.72 \pm 0.16	57.69 \pm 0.30	33.14 \pm 0.86
	GAIN (Multi-Krum)	66.79 \pm 1.08	63.04 \pm 0.14	57.15 \pm 0.19	59.94 \pm 0.32	64.07 \pm 1.38	61.92 \pm 0.04
	Bulyan	62.28 \pm 0.84	59.84 \pm 1.09	48.04 \pm 2.22	48.97 \pm 1.87	59.94 \pm 0.51	60.67 \pm 0.07
	GAIN (Bulyan)	66.76 \pm 0.72	62.28 \pm 0.32	57.44 \pm 0.39	58.81 \pm 0.05	65.00 \pm 0.08	62.76 \pm 0.14
ImageNet-12	Median	55.93 \pm 0.55	58.14 \pm 0.18	46.67 \pm 1.01	49.07 \pm 1.19	58.40 \pm 0.03	43.62 \pm 1.72
	GAIN (Median)	66.28 \pm 0.41	62.34 \pm 1.10	60.74 \pm 1.24	59.26 \pm 0.31	64.78 \pm 2.10	62.24 \pm 0.51
	RFA	61.12 \pm 1.26	61.31 \pm 1.68	49.49 \pm 1.33	53.04 \pm 0.13	61.92 \pm 0.67	63.97 \pm 0.93
	GAIN (RFA)	66.92 \pm 1.58	63.88 \pm 0.94	61.41 \pm 0.02	59.42 \pm 0.64	67.02 \pm 0.54	66.67 \pm 0.38
	DnC	54.94 \pm 0.04	5.59 \pm 0.06	58.01 \pm 1.52	58.11 \pm 0.41	60.42 \pm 1.60	59.99 \pm 0.50
	GAIN (DnC)	65.19 \pm 1.63	63.01 \pm 0.27	64.42 \pm 0.19	65.03 \pm 1.23	65.38 \pm 1.68	65.03 \pm 0.04
	RBTM	60.06 \pm 1.76	60.44 \pm 0.37	55.77 \pm 0.82	57.50 \pm 0.10	63.91 \pm 0.78	56.19 \pm 1.05
	GAIN (RBTM)	66.99 \pm 0.38	61.92 \pm 1.22	59.87 \pm 0.72	59.81 \pm 1.34	64.94 \pm 0.72	63.40 \pm 0.97

Evaluated attacks. We consider six representative attacks BitFlip [19], LabelFlip [19], LIE [31], Min-Max [17], Min-Sum [17] and IPM [32]. The detailed hyperparameter setting of the attacks are shown in Table 5 in Appendix C.

Baselines. We consider 6 robust AGRs: [4], Bulyan [5], Median [8], RFA [18], DnC [17], RBTM [25]. Among the above six defenses, Bulyan, Median, and RBTM are conservative, and Multi-Krum, RFA, and DnC are radical. We compare each AGR with its variant with GAIN. The detailed hyperparameter settings of the robust AGRs are listed in Table 6 in Appendix C.

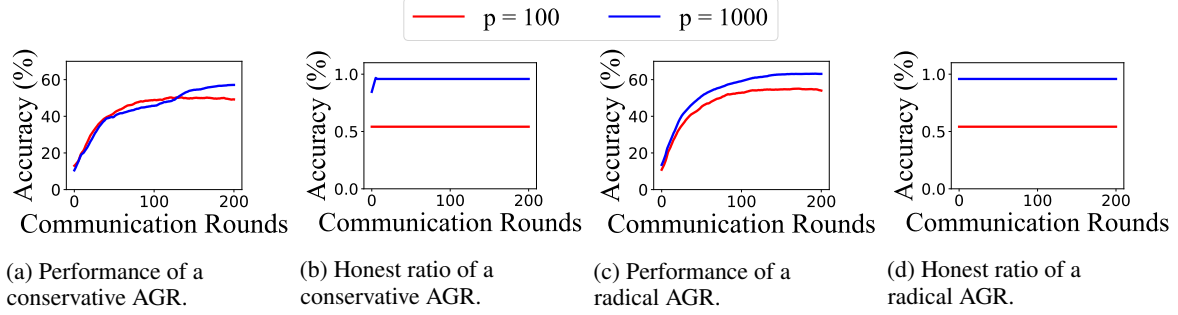


Figure 2: The behaviors of a conservative AGR (Bulyan) and a radical AGR (Multi-Krum) across sub-vector number $p = 100, 1000$ under the attack of 20% Byzantines in the non-IID setting on CIFAR-10 dataset. More detailed setups are covered in Appendix C.2.

Evaluation. We use top-1 accuracy, i.e., the proportion of correctly predicted testing samples to total testing samples, to evaluate the performance of global models. We run each experiment for 5 times and report the mean and standard deviation of the highest accuracy during the training process.

Other settings. We utilize AlexNet [33], SqueezeNet [34], ResNet-18 [35] and a four-layer CNN [30] for CIFAR-10, CIFAR-100, ImageNet-12 and FEMNIST, respectively. The number of Byzantine clients of all datasets is set to $f = 0.2 \cdot n$. For the partition of set $\{1, \dots, d\}$, we randomly partition $\{1, \dots, d\}$ into p disjoint subsets with equal size. Please refer to Table 4 in Appendix C for more details.

7.2 Experiment Results

Main results. Table 1 illustrates the results of different defenses against popular attacks on CIFAR-10, CIFAR-100, ImageNet-12 and FEMNIST. From these tables, we observe that:

- (1) Integrating current defenses into our GAIN generally outperform all their original versions on all datasets, which verifies the efficacy of our proposed GAIN. For example, GAIN improves the accuracy of Median by 15.93% under Min-Sum attack on CIFAR-10.
- (2) The improvement of DnC+GAIN to DnC is relatively mild on CIFAR-10. Our interpretation is that when the dataset is relatively small and simple, DnC is capable of obtaining a rational gradient estimation. Nevertheless, on larger and more complex datasets, i.e., FEMNIST and ImageNet-12, DnC fails to achieve satisfactory performance under Byzantine attacks.
- (3) We find that although RFA collapses on FEMNIST, integrating into our GAIN can still improve it to satisfactory performance. Our illustration is that although the aggregated gradient of RFA deviates from the optimal gradient, it can still assist in identifying honest gradients when combined with GAIN. As a result, GAIN-RFA is still effective on FEMNIST.
- (4) Note that the improvement of GAIN on conservative methods is greater. We contribute this phenomenon to the gradient heterogeneity due to non-IID data. Excluding honest gradients deviates the aggregated gradients from the average of honest gradients, thus degrading the performance of conservative methods. When the non-IID degree increases, the gradient heterogeneity increases. As a result, the impact of excluding honest gradients may even be larger than incorporating Byzantine gradients. Therefore, the improvement on the conservative AGRs is greater.

Number of sub-vectors. We study the influence of sub-vector number p on the heterogeneous CIFAR-10 dataset. Figure 2 shows the performance and honest ratio of a conservative AGR (Bulyan) and a radical AGR (Multi-Krum) across $p = \{100, 1000\}$. The results show that for both conservative and radical AGRs, GAIN with a larger sub-vector number p can select a higher proportion of honest clients and achieve better performance. When the sub-vector number p increases, our GAIN can better handle the identification failure and the integrity failure, which corresponds to our theoretical analysis in Sec. 6.

Results on different levels of non-IID. We discuss the impact of non-IID level of data distributions. We modify the concentration parameter β to change the non-IID level. A smaller β implies a higher non-IID level. Table 2 demonstrates the accuracy of different defenses under LIE attack on CIFAR-10 dataset across $\beta = \{0.3, 0.7\}$. Other setups follow the default setup of the main experiments as illustrated in Sec. 7.1 and Appendix C. As shown in Table 2, all the

existing AGRs that combined with GAIN achieve better performances than their original versions, which validates that integrating into our GAIN can effectively defend against Byzantine attacks under different non-IID levels. Moreover, when the level of non-IID is higher, the improvement on robust AGRs is more significant. The results further confirm that our GAIN can overcome the failures aggravated under a higher non-IID level.

Table 2: Accuracy (mean \pm std) of different defenses against LIE attack under different non-IID levels on CIFAR-10. A smaller β implies a higher non-IID level.

β	Multi-Krum	Multi-Krum+GAIN	Bulyan	Bulyan+GAIN	Median	Median+GAIN
0.3	12.19 \pm 1.04	52.80 \pm 0.74	28.16 \pm 0.44	42.81 \pm 0.63	25.62 \pm 0.83	40.97 \pm 0.89
0.7	31.01 \pm 0.54	55.64 \pm 0.60	44.72 \pm 1.43	51.29 \pm 0.35	34.04 \pm 0.29	53.34 \pm 0.08
β	RFA	RFA+GAIN	DnC	DnC+GAIN	RBTM	RBTM+GAIN
0.3	20.08 \pm 0.13	48.77 \pm 0.84	59.99 \pm 1.81	60.21 \pm 0.62	37.67 \pm 0.18	49.27 \pm 0.05
0.7	18.11 \pm 0.24	53.25 \pm 1.41	62.15 \pm 0.73	62.48 \pm 0.52	48.43 \pm 0.22	52.25 \pm 1.16

Results on different number of Byzantine clients. We also conduct experiments across different number of Byzantine clients. Other setups follow the default setup of the main experiments in Sec. 7.1 and Appendix C. Table 3 demonstrates the results of different defenses under LIE attack across $f = \{5, 15\}$ Byzantine clients on CIFAR-10 dataset. As shown in Table 3, our GAIN outperforms the corresponding baselines across all Byzantine client numbers.

Table 3: Accuracy (mean \pm std) of different defenses against LIE attack with different Byzantine client numbers $f = \{5, 15\}$ on CIFAR-10. The number of total clients is $n = 50$.

f	Multi-Krum	Multi-Krum+GAIN	Bulyan	Bulyan+GAIN	Median	Median+GAIN
5	41.65 \pm 1.78	61.24 \pm 0.01	56.28 \pm 1.44	58.27 \pm 0.17	46.91 \pm 1.36	57.69 \pm 1.81
15	10.00 \pm 0.00	34.70 \pm 0.28	10.00 \pm 0.00	31.67 \pm 0.19	18.85 \pm 1.54	30.95 \pm 0.42
f	RFA	RFA+GAIN	DnC	DnC+GAIN	RBTM	RBTM+GAIN
5	22.37 \pm 1.00	58.06 \pm 1.29	62.27 \pm 0.04	63.14 \pm 0.20	55.92 \pm 0.10	59.72 \pm 0.16
15	16.16 \pm 0.14	40.37 \pm 0.26	57.28 \pm 1.37	60.14 \pm 1.64	34.93 \pm 1.36	35.78 \pm 1.51

Results on different number of clients. We further analyze the efficacy of our GAIN under different number of clients. Detailed setups can be found in Appendix E. And the experimental results are shown in Table 7 in Appendix E. All results demonstrate that AGRs that combine with our GAIN consistently outperform all their original versions, which validates that integrating with our GAIN can effectively defend against Byzantine across different number of clients.

8 Conclusion

In this work, we identify two root causes of performance degradation of robust AGRs in the non-IID setting. The first cause is the integrity failure of conservative AGRs. Conservative AGRs aggregate only few honest gradients, which is unreliable due to the gradient heterogeneity in the non-IID setting. The second cause is the identification failure of radical AGRs. Radical AGRs inevitably introduce Byzantine gradients into aggregation due to the curse of dimensionality aggravated by the non-IIDness. Both failures result in a sharp deviation of the aggregated gradient. Motivated by the above discoveries, we propose a novel GrAdient decomposItioN (GAIN) method that can be combined with most existing defenses and overcome both failures. We also provide convergence analysis for integrating existing robust AGRs into GAIN. Empirical studies on three real-world datasets justify the efficacy of our proposed GAIN.

References

- [1] Brendan McMahan, Eider Moore, Daniel Ramage, Seth Hampson, and Blaise Aguera y Arcas. Communication-efficient learning of deep networks from decentralized data. In *Artificial intelligence and statistics*, pages 1273–1282. PMLR, 2017.
- [2] Chuhan Wu, Fangzhao Wu, Lingjuan Lyu, Yongfeng Huang, and Xing Xie. Communication-efficient federated learning via knowledge distillation. *Nature communications*, 13(1):2032, 2022.
- [3] Lingjuan Lyu, Jiangshan Yu, Karthik Nandakumar, Yitong Li, Xingjun Ma, Jiong Jin, Han Yu, and Kee Siong Ng. Towards fair and privacy-preserving federated deep models. *IEEE Transactions on Parallel and Distributed Systems*, 31(11):2524–2541, 2020.
- [4] Peva Blanchard, El Mahdi El Mhamdi, Rachid Guerraoui, and Julien Stainer. Machine learning with adversaries: Byzantine tolerant gradient descent. *Advances in Neural Information Processing Systems*, 30, 2017.
- [5] Rachid Guerraoui, Sébastien Rouault, et al. The hidden vulnerability of distributed learning in byzantium. In *International Conference on Machine Learning*, pages 3521–3530. PMLR, 2018.
- [6] Lingjuan Lyu, Han Yu, Xingjun Ma, Chen Chen, Lichao Sun, Jun Zhao, Qiang Yang, and S Yu Philip. Privacy and robustness in federated learning: Attacks and defenses. *IEEE transactions on neural networks and learning systems*, 2022.
- [7] Gan Sun, Yang Cong, Jiahua Dong, Qiang Wang, Lingjuan Lyu, and Ji Liu. Data poisoning attacks on federated machine learning. *IEEE Internet of Things Journal*, 9(13):11365–11375, 2021.
- [8] Dong Yin, Yudong Chen, Ramchandran Kannan, and Peter Bartlett. Byzantine-robust distributed learning: Towards optimal statistical rates. In *International Conference on Machine Learning*, pages 5650–5659. PMLR, 2018.
- [9] Jeremy Bernstein, Yu-Xiang Wang, Kamyar Azizzadenesheli, and Animashree Anandkumar. signsgd: Compressed optimisation for non-convex problems. In *International Conference on Machine Learning*, pages 560–569. PMLR, 2018.
- [10] Avishek Ghosh, Justin Hong, Dong Yin, and Kannan Ramchandran. Robust federated learning in a heterogeneous environment. *arXiv preprint arXiv:1906.06629*, 2019.
- [11] Sai Praneeth Karimireddy, Satyen Kale, Mehryar Mohri, Sashank Reddi, Sebastian Stich, and Ananda Theertha Suresh. Scaffold: Stochastic controlled averaging for federated learning. In *International Conference on Machine Learning*, pages 5132–5143. PMLR, 2020.
- [12] Peter Kairouz, H Brendan McMahan, Brendan Avent, Aurélien Bellet, Mehdi Bennis, Arjun Nitin Bhagoji, Kallista Bonawitz, Zachary Charles, Graham Cormode, Rachel Cummings, et al. Advances and open problems in federated learning. *Foundations and Trends® in Machine Learning*, 14(1–2):1–210, 2021.
- [13] Sai Praneeth Karimireddy, Lie He, and Martin Jaggi. Byzantine-robust learning on heterogeneous datasets via bucketing. In *International Conference on Learning Representations*, 2022.
- [14] Anish Acharya, Abolfazl Hashemi, Prateek Jain, Sujay Sanghavi, Inderjit S Dhillon, and Ufuk Topcu. Robust training in high dimensions via block coordinate geometric median descent. In *International Conference on Artificial Intelligence and Statistics*, pages 11145–11168. PMLR, 2022.
- [15] Tian Li, Anit Kumar Sahu, Manzil Zaheer, Maziar Sanjabi, Ameet Talwalkar, and Virginia Smith. Federated optimization in heterogeneous networks. *Proceedings of Machine Learning and Systems*, 2:429–450, 2020.
- [16] Ilias Diakonikolas, Gautam Kamath, Daniel M Kane, Jerry Li, Ankur Moitra, and Alistair Stewart. Being robust (in high dimensions) can be practical. In *International Conference on Machine Learning*, pages 999–1008. PMLR, 2017.
- [17] Virat Shejwalkar and Amir Houmansadr. Manipulating the byzantine: Optimizing model poisoning attacks and defenses for federated learning. In *NDSS*, 2021.
- [18] Krishna Pillutla, Sham M Kakade, and Zaid Harchaoui. Robust aggregation for federated learning. *arXiv preprint arXiv:1912.13445*, 2019.
- [19] Zeyuan Allen-Zhu, Faeze Ebrahimiaghazani, Jerry Li, and Dan Alistarh. Byzantine-resilient non-convex stochastic gradient descent. In *International Conference on Learning Representations*, 2020.
- [20] Sai Praneeth Karimireddy, Lie He, and Martin Jaggi. Learning from history for byzantine robust optimization. In *International Conference on Machine Learning*, pages 5311–5319. PMLR, 2021.

- [21] Sadegh Farhadkhani, Rachid Guerraoui, Nirupam Gupta, Rafael Pinot, and John Stephan. Byzantine machine learning made easy by resilient averaging of momentums. In *Proceedings of the 39th International Conference on Machine Learning*, volume 162 of *Proceedings of Machine Learning Research*, pages 6246–6283. PMLR, 17–23 Jul 2022.
- [22] Chen Chen, Lingjuan Lyu, Yuchen Liu, Fangzhao Wu, Chaochao Chen, and Gang Chen. Byzantine-resilient federated learning via gradient memorization.
- [23] Jungwuk Park, Dong-Jun Han, Minseok Choi, and Jaekyun Moon. Sageflow: Robust federated learning against both stragglers and adversaries. *Advances in Neural Information Processing Systems*, 34:840–851, 2021.
- [24] Deepesh Data and Suhas Diggavi. Byzantine-resilient high-dimensional sgd with local iterations on heterogeneous data. In *International Conference on Machine Learning*, pages 2478–2488. PMLR, 2021.
- [25] El Mahdi El-Mhamdi, Sadegh Farhadkhani, Rachid Guerraoui, Arsany Guirguis, Lê-Nguyên Hoang, and Sébastien Rouault. Collaborative learning in the jungle (decentralized, byzantine, heterogeneous, asynchronous and nonconvex learning). *Advances in Neural Information Processing Systems*, 34:25044–25057, 2021.
- [26] Alex Krizhevsky et al. Learning multiple layers of features from tiny images. 2009.
- [27] Jianyu Wang, Zachary Charles, Zheng Xu, Gauri Joshi, H Brendan McMahan, Maruan Al-Shedivat, Galen Andrew, Salman Avestimehr, Katharine Daly, Deepesh Data, et al. A field guide to federated optimization. *arXiv preprint arXiv:2107.06917*, 2021.
- [28] El Mahdi El Mhamdi, Rachid Guerraoui, and Sébastien Louis Alexandre Rouault. Distributed momentum for byzantine-resilient stochastic gradient descent. In *9th International Conference on Learning Representations (ICLR)*, number CONF, 2021.
- [29] Olga Russakovsky, Jia Deng, Hao Su, Jonathan Krause, Sanjeev Satheesh, Sean Ma, Zhiheng Huang, Andrej Karpathy, Aditya Khosla, Michael Bernstein, et al. Imagenet large scale visual recognition challenge. *International journal of computer vision*, 115(3):211–252, 2015.
- [30] Sebastian Caldas, Sai Meher Karthik Duddu, Peter Wu, Tian Li, Jakub Konečný, H Brendan McMahan, Virginia Smith, and Ameet Talwalkar. Leaf: A benchmark for federated settings. *arXiv preprint arXiv:1812.01097*, 2018.
- [31] Gilad Baruch, Moran Baruch, and Yoav Goldberg. A little is enough: Circumventing defenses for distributed learning. *Advances in Neural Information Processing Systems*, 32, 2019.
- [32] Cong Xie, Oluwasanmi Koyejo, and Indranil Gupta. Fall of empires: Breaking byzantine-tolerant sgd by inner product manipulation. In *Uncertainty in Artificial Intelligence*, pages 261–270. PMLR, 2020.
- [33] Alex Krizhevsky, Ilya Sutskever, and Geoffrey E Hinton. Imagenet classification with deep convolutional neural networks. *Communications of the ACM*, 60(6):84–90, 2017.
- [34] Forrest N Iandola, Song Han, Matthew W Moskewicz, Khalid Ashraf, William J Dally, and Kurt Keutzer. Squeezenet: Alexnet-level accuracy with 50x fewer parameters and < 0.5 mb model size. *arXiv preprint arXiv:1602.07360*, 2016.
- [35] Kaiming He, Xiangyu Zhang, Shaoqing Ren, and Jian Sun. Deep residual learning for image recognition. In *Proceedings of the IEEE conference on computer vision and pattern recognition*, pages 770–778, 2016.
- [36] Ge Yang and Samuel Schoenholz. Mean field residual networks: On the edge of chaos. *Advances in neural information processing systems*, 30, 2017.
- [37] Jie Peng, Zhaoxian Wu, Qing Ling, and Tianyi Chen. Byzantine-robust variance-reduced federated learning over distributed non-iid data. *Information Sciences*, 616:367–391, 2022.
- [38] Mikhail Yurochkin, Mayank Agarwal, Soumya Ghosh, Kristjan Greenewald, Nghia Hoang, and Yasaman Khazaeni. Bayesian nonparametric federated learning of neural networks. In *International Conference on Machine Learning*, pages 7252–7261, 2019.
- [39] Qinbin Li, Yiqun Diao, Quan Chen, and Bingsheng He. Federated learning on non-iid data silos: An experimental study. *arXiv preprint arXiv:2102.02079*, 2021.

A Setups for Experiments in Sec. 4

The experiments are conducted on CIFAR-10 [26].

For both IID and non-IID settings, the number of client is set to $n = 50$. For IID data distribution, all 50,000 samples are randomly partitioned into 50 clients each containing 1,000 samples. For non-IID data distribution, the samples are partitioned in a Dirichlet manner with concentration parameter $\beta = 0.5$. Please refer to Sec. 7.1 for the details of Dirichlet partition.

The number of Byzantine clients is set to $f = 10$. LIE [31] attack with $z = 1.5$ considered.

We use AlexNet [33] as the model architecture. The number of communication rounds is set to 500. In each communication round, all client participate in the training.

For local training, the number of local epochs is set to 1, batch size is set to 64, the optimizer is set to SGD. For SGD optimizer, learning rate is set to 0.1, momentum is set to 0.5, weight decay coefficient is set to 0.0001. We also adopt gradient clipping with clipping norm 2.

Two defenses are considered: a radical AGR Multi-Krum [4] and a conservative AGR Bulyan [5].

B Convergence Analysis

In this section, we provide the proof for our convergence results in Sec. 6 and the comparison of our convergence results with recent works.

We first restate the assumptions, the definition and the proposition for the integrity of this section. [Unbiased Estimator] The stochastic gradients sampled from any local data distribution are unbiased estimators of local gradients over \mathbb{R}^d for all clients, i.e.,

$$\begin{aligned} \mathbb{E}_{\xi_i^t}[\nabla \mathcal{L}_i(\mathbf{w}; \xi_i^t)] &= \nabla \mathcal{L}_i(\mathbf{w}), \\ \forall \mathbf{w} \in \mathbb{R}^d, i \in [n], t \in \mathbb{N}^+. \end{aligned} \quad (13)$$

[Bounded Variance] The variance of stochastic gradients sampled from any local data distribution is uniformly bounded over \mathbb{R}^d for all clients, i.e., there exists $\sigma \geq 0$ such that

$$\begin{aligned} \mathbb{E}\|\nabla \mathcal{L}_i(\mathbf{w}; \xi_i^t) - \nabla \mathcal{L}_i(\mathbf{w})\|^2 &\leq \sigma^2, \\ \forall \mathbf{w} \in \mathbb{R}^d, i \in [n], t \in \mathbb{N}^+. \end{aligned} \quad (14)$$

[Gradient Dissimilarity] The difference between the local gradients and the global gradient is uniformly bounded over \mathbb{R}^d for all clients, i.e., there exists $\kappa \geq 0$ such that

$$\|\nabla \mathcal{L}_i(\mathbf{w}) - \nabla \mathcal{L}(\mathbf{w})\|^2 \leq \kappa^2, \quad \forall \mathbf{w} \in \mathbb{R}^d, i \in [n]. \quad (15)$$

[Lipschitz Smoothness] The loss function is L -Lipschitz smooth with respect over \mathbb{R}^d , i.e.,

$$\begin{aligned} \|\nabla \mathcal{L}(\mathbf{w}) - \nabla \mathcal{L}(\mathbf{w}')\| &\leq L\|\mathbf{w} - \mathbf{w}'\|, \\ \forall \mathbf{w}, \mathbf{w}' \in \mathbb{R}^d. \end{aligned} \quad (16)$$

Definition 1 ((f, λ) -resilient). For $f \leq n$ and real value λ , an AGR \mathcal{A} is called (f, λ) -resilient if for any input $\{\mathbf{x}_1, \dots, \mathbf{x}_n\}$ and any set $\mathcal{S} \subseteq [n]$ of size $n - f$, the output of \mathcal{A} satisfies:

$$\|\mathcal{A}(\mathbf{x}_1, \dots, \mathbf{x}_n) - \bar{\mathbf{x}}_{\mathcal{S}}\| \leq \lambda \max_{i, i' \in \mathcal{S}} \|\mathbf{x}_i - \mathbf{x}_{i'}\|, \quad (17)$$

where $\bar{\mathbf{x}}_{\mathcal{S}} = \sum_{i \in \mathcal{S}} \mathbf{x}_i / |\mathcal{S}|$.

Suppose Sec. 6 hold, and let $\eta = 1/2L$. Given an (f, λ) -resilient robust AGR \mathcal{A} , we start from \mathbf{w}^0 and run GAIN for T communication rounds, it satisfies

$$\mathcal{L}(\mathbf{w}^0) \geq \frac{3}{16L} \sum_{t=1}^T (\|\nabla \mathcal{L}(\mathbf{w}^t)\|^2 - e^2), \quad (18)$$

where

$$e^2 = \mathcal{O}((\kappa^2 + \sigma^2)(1 + \frac{n - f + 1}{p})(1 + c^2 + \frac{1}{n - f})\frac{f^2}{(n - f)^2}). \quad (19)$$

B.1 Proof for Sec. 6

Lemma 1. For positive integer n , $f \leq n$ and real value λ , AGR \mathcal{A} is (f, λ) -resilient. Then for any set of random variables $\{\mathbf{x}_1, \dots, \mathbf{x}_n\}$ and $\mathcal{S} \subseteq [n]$ of size $n - f$ that satisfies,

$$\mathbb{E}[\|\mathbf{x}_i - \mathbf{x}_{i'}\|^2] \leq \rho^2, \quad \forall i, i' \in \mathcal{H} \quad (20)$$

we have

$$\mathbb{E}[\|\mathcal{A}(\mathbf{x}_1, \dots, \mathbf{x}_n) - \mathbf{x}_{\mathcal{S}}\|^2] \leq 4\lambda^2 \cdot \frac{(n - f - 1)^2}{n - f} \cdot \rho^2, \quad (21)$$

where $\mathbf{x}_{\mathcal{S}} = \sum_{i \in \mathcal{S}} \mathbf{x}_i / |\mathcal{S}|$.

Proof. Since \mathcal{A} is (f, λ) -resilient, we have

$$\mathbb{E}[\|\mathcal{A}(\mathbf{x}_1, \dots, \mathbf{x}_n) - \bar{\mathbf{x}}_{\mathcal{S}}\|^2] \leq \mathbb{E}[\lambda^2 \max_{i, i' \in \mathcal{S}} \|\mathbf{x}_i - \mathbf{x}_{i'}\|^2] = \lambda^2 \mathbb{E}[\max_{i, i' \in \mathcal{S}} \|\mathbf{x}_i - \mathbf{x}_{i'}\|^2]. \quad (22)$$

Then we bound $\max_{i, i' \in \mathcal{S}} \|\mathbf{x}_i - \mathbf{x}_{i'}\|^2$ as follows.

$$\max_{i, i' \in \mathcal{S}} \|\mathbf{x}_i - \mathbf{x}_{i'}\|^2 \leq \max_{i, i' \in \mathcal{S}} 2(\|\mathbf{x}_i - \mathbf{x}_{\mathcal{S}}\|^2 + \|\mathbf{x}_{\mathcal{S}} - \mathbf{x}_{i'}\|^2) \quad (23)$$

$$\leq \max_{i, i' \in \mathcal{S}} 2\|\mathbf{x}_i - \mathbf{x}_{\mathcal{S}}\|^2 + \max_{i, i' \in \mathcal{S}} 2\|\mathbf{x}_{\mathcal{S}} - \mathbf{x}_{i'}\|^2 \quad (24)$$

$$= 4 \max_{i \in \mathcal{S}} \|\mathbf{x}_i - \mathbf{x}_{\mathcal{S}}\|^2 \quad (25)$$

$$\leq 4 \sum_{i \in \mathcal{S}} \|\mathbf{x}_i - \mathbf{x}_{\mathcal{S}}\|^2 \quad (26)$$

Here Inequality (23) comes from the Cauchy inequality.

We further bound $\|\mathbf{x}_i - \mathbf{x}_{\mathcal{S}}\|^2$ for all $i \in \mathcal{S}$ as follows.

$$\|\mathbf{x}_i - \mathbf{x}_{\mathcal{S}}\|^2 = \frac{1}{(n - f)^2} \left\| \sum_{i' \in \mathcal{S} \setminus \{i\}} (\mathbf{x}_i - \mathbf{x}_{i'}) \right\|^2 \quad (27)$$

$$\leq \frac{1}{(n - f)^2} \cdot (n - f - 1) \sum_{i' \in \mathcal{S} \setminus \{i\}} \|\mathbf{x}_i - \mathbf{x}_{i'}\|^2 \quad (28)$$

$$= \frac{n - f - 1}{(n - f)^2} \sum_{i' \in \mathcal{S} \setminus \{i\}} \|\mathbf{x}_i - \mathbf{x}_{i'}\|^2. \quad (29)$$

Here Equation (28) comes from the Cauchy inequality.

Combine Equations (22) and (29) and Inequality (26) and we have

$$\mathbb{E}[\|\mathcal{A}(\mathbf{x}_1, \dots, \mathbf{x}_n) - \mathbf{x}_{\mathcal{S}}\|^2] \leq \lambda^2 \mathbb{E}[\max_{i, i' \in \mathcal{S}} \|\mathbf{x}_i - \mathbf{x}_{i'}\|^2] \quad (30)$$

$$\leq \lambda^2 \mathbb{E}[4 \sum_{i \in \mathcal{S}} \|\mathbf{x}_i - \mathbf{x}_{\mathcal{S}}\|^2] \quad (31)$$

$$\leq \lambda^2 \mathbb{E}[4 \sum_{i \in \mathcal{S}} \frac{n - f - 1}{(n - f)^2} \sum_{i' \in \mathcal{S} \setminus \{i\}} \|\mathbf{x}_i - \mathbf{x}_{i'}\|^2] \quad (32)$$

$$\leq 4\lambda^2 \cdot \frac{n - f - 1}{(n - f)^2} \sum_{i, i' \in \mathcal{S}, i \neq i'} \mathbb{E}[\|\mathbf{x}_i - \mathbf{x}_{i'}\|^2] \quad (33)$$

$$\leq 4\lambda^2 \cdot \frac{n - f - 1}{(n - f)^2} \cdot (n - f)(n - f - 1)\rho^2 \quad (34)$$

$$= 4\lambda^2 \cdot \frac{(n - f - 1)^2}{n - f} \cdot \rho^2 \quad (35)$$

□

We state and prove the following lemma for the proof of Lemma 3.

Lemma 2. *For any random vector \mathbf{X} , we have*

$$\text{Var}[\|\mathbf{X}\|] \leq \mathbb{E}\|\mathbf{X} - \mathbb{E}\mathbf{X}\|^2. \quad (36)$$

Proof. From the definition of variance, we have

$$\text{Var}[\|\mathbf{X}\|] = \mathbb{E}(\|\mathbf{X}\| - \mathbb{E}\|\mathbf{X}\|)^2 \quad (37)$$

$$= \mathbb{E}(\|\mathbf{X}\| - \|\mathbb{E}\mathbf{X}\|)^2 - (\|\mathbb{E}\mathbf{X}\| - \mathbb{E}\|\mathbf{X}\|)^2 \quad (38)$$

$$\leq \mathbb{E}(\|\mathbf{X}\| - \|\mathbb{E}\mathbf{X}\|)^2 \quad (39)$$

$$\leq \mathbb{E}\|\mathbf{X} - \mathbb{E}\mathbf{X}\|^2. \quad (40)$$

The second inequality comes from triangular inequality. \square

Lemma 3 (Aggregation error). *Suppose Sec. 6 hold. Given an (f, λ) -resilient robust AGR \mathcal{A} , for any $t > 0$, it satisfies*

$$\mathbb{E}[\|\hat{\mathbf{g}} - \bar{\mathbf{g}}\|^2] \leq \mathcal{O}((\kappa^2 + \sigma^2)(1 + \frac{n-f+1}{p})(1 + c^2 + \frac{1}{n-f})\frac{f^2}{(n-f)^2}) \quad (41)$$

Proof. We rewrite $\hat{\mathbf{g}}$ as follows.

$$\hat{\mathbf{g}} = \frac{1}{n-f} \sum_{i \in \mathcal{I}} \mathbf{g}_i = \frac{1}{n-f} (\sum_{h \in \tilde{\mathcal{H}}} \mathbf{g}_h + \sum_{b \in \tilde{\mathcal{B}}} \mathbf{g}_b) = \frac{|\tilde{\mathcal{H}}|}{n-f} \mathbf{g}_{\tilde{\mathcal{H}}} + \frac{|\tilde{\mathcal{B}}|}{n-f} \mathbf{g}_{\tilde{\mathcal{B}}}. \quad (42)$$

Here $\tilde{\mathcal{H}} = \mathcal{H} \cap \mathcal{I}$, $\tilde{\mathcal{B}} = \mathcal{B} \cap \mathcal{I}$, and $\mathbf{g}_{\mathcal{S}} = \sum_{i \in \mathcal{S}} \mathbf{g}_i / |\mathcal{S}|$ for all $\mathcal{S} \in [n]$.

Then, we can bound $\mathbb{E}\|\hat{\mathbf{g}} - \bar{\mathbf{g}}\|^2$ as follows

$$\mathbb{E}[\|\hat{\mathbf{g}} - \bar{\mathbf{g}}\|^2] = \mathbb{E}[\|\frac{|\tilde{\mathcal{H}}|}{n-f} \mathbf{g}_{\tilde{\mathcal{H}}} + \frac{|\tilde{\mathcal{B}}|}{n-f} \mathbf{g}_{\tilde{\mathcal{B}}} - \bar{\mathbf{g}}\|^2] \quad (43)$$

$$= \mathbb{E}[\|\frac{|\tilde{\mathcal{H}}|}{n-f} (\mathbf{g}_{\tilde{\mathcal{H}}} - \bar{\mathbf{g}}) + \frac{|\tilde{\mathcal{B}}|}{n-f} (\mathbf{g}_{\tilde{\mathcal{B}}} - \bar{\mathbf{g}})\|^2] \quad (44)$$

$$\leq \frac{2|\tilde{\mathcal{H}}|^2}{(n-f)^2} \mathbb{E}[\|\mathbf{g}_{\tilde{\mathcal{H}}} - \bar{\mathbf{g}}\|^2] + \frac{2|\tilde{\mathcal{B}}|^2}{(n-f)^2} \mathbb{E}[\|\mathbf{g}_{\tilde{\mathcal{B}}} - \bar{\mathbf{g}}\|^2]. \quad (45)$$

We bound $\mathbb{E}[\|\mathbf{g}_{\tilde{\mathcal{H}}} - \bar{\mathbf{g}}\|^2]$ as follows.

$$\mathbb{E}[\|\mathbf{g}_{\tilde{\mathcal{H}}} - \bar{\mathbf{g}}\|^2] = \mathbb{E}[\|(\mathbf{g}_{\tilde{\mathcal{H}}} - \bar{\mathbf{g}}_{\tilde{\mathcal{H}}}) + (\bar{\mathbf{g}}_{\tilde{\mathcal{H}}} - \bar{\mathbf{g}})\|^2] \quad (46)$$

$$= \mathbb{E}[\|\mathbf{g}_{\tilde{\mathcal{H}}} - \bar{\mathbf{g}}_{\tilde{\mathcal{H}}}\|^2] + \|\bar{\mathbf{g}}_{\tilde{\mathcal{H}}} - \bar{\mathbf{g}}\|^2 \quad (47)$$

$$\leq \frac{\sigma^2}{|\tilde{\mathcal{H}}|} + \kappa^2, \quad (48)$$

where $\bar{\mathbf{g}}_{\tilde{\mathcal{H}}} = \mathbb{E}[\mathbf{g}_{\tilde{\mathcal{H}}}]$.

Then we consider $\mathbb{E}[\|\mathbf{g}_{\tilde{\mathcal{B}}} - \bar{\mathbf{g}}\|^2]$. According to the law of total expectation, we have

$$\mathbb{E}[\|\mathbf{g}_{\tilde{\mathcal{B}}} - \bar{\mathbf{g}}\|^2] = \sum_{\tilde{f}=0}^f \mathbb{E}[\|\mathbf{g}_{\tilde{\mathcal{B}}} - \bar{\mathbf{g}}\|^2 \mid |\tilde{\mathcal{B}}| = \tilde{f}] \Pr(|\tilde{\mathcal{B}}| = \tilde{f}). \quad (49)$$

For all parameter group $q \in [p]$ and $i, j \in \mathcal{H}$, we have

$$\mathbb{E}[\|\mathbf{g}_i^{(q)} - \mathbf{g}_j^{(q)}\|^2] = \mathbb{E}[\|(\mathbf{g}_i^{(q)} - \bar{\mathbf{g}}_i^{(q)}) + (\bar{\mathbf{g}}_i^{(q)} - \bar{\mathbf{g}}^{(q)}) + (\bar{\mathbf{g}}^{(q)} - \bar{\mathbf{g}}_j^{(q)}) + (\bar{\mathbf{g}}_j^{(q)} - \mathbf{g}_j^{(q)})\|^2] \quad (50)$$

$$= \mathbb{E}[\|\mathbf{g}_i^{(q)} - \bar{\mathbf{g}}_i^{(q)}\|^2] + \|\bar{\mathbf{g}}_i^{(q)} - \bar{\mathbf{g}}^{(q)}\|^2 + \|\bar{\mathbf{g}}^{(q)} - \bar{\mathbf{g}}_j^{(q)}\|^2 + \mathbb{E}[\|\bar{\mathbf{g}}_j^{(q)} - \mathbf{g}_j^{(q)}\|^2] \quad (51)$$

$$+ 2\langle \bar{\mathbf{g}}_i^{(q)} - \bar{\mathbf{g}}^{(q)}, \bar{\mathbf{g}}^{(q)} - \bar{\mathbf{g}}_j^{(q)} \rangle \quad (52)$$

$$\leq \mathbb{E}[\|\mathbf{g}_i^{(q)} - \bar{\mathbf{g}}_i^{(q)}\|^2] + \|\bar{\mathbf{g}}_i^{(q)} - \bar{\mathbf{g}}^{(q)}\|^2 + \|\bar{\mathbf{g}}^{(q)} - \bar{\mathbf{g}}_j^{(q)}\|^2 + \mathbb{E}[\|\bar{\mathbf{g}}_j^{(q)} - \mathbf{g}_j^{(q)}\|^2] \quad (52)$$

$$+ 2\|\bar{\mathbf{g}}_i^{(q)} - \bar{\mathbf{g}}^{(q)}\| \cdot \|\bar{\mathbf{g}}^{(q)} - \bar{\mathbf{g}}_j^{(q)}\| \quad (53)$$

$$\leq 2\sigma^2 + 4\kappa^2$$

Here Equation (51) is due to the independence of $\mathbf{g}_i^{(q)}$ and $\mathbf{g}_j^{(q)}$, Inequality (52) comes from the Cauchy inequality, and Inequality (53) follows Sec. 6.

Then according to the Lemma 1, we have

$$\mathbb{E}[\|\hat{\mathbf{g}}^{(q)} - \mathbf{g}^{(q)}\|^2] \leq c^2 \max_{i,j \in \mathcal{H}} \mathbb{E}[\|\mathbf{g}_i^{(q)} - \mathbf{g}_j^{(q)}\|^2] \leq c^2(2\sigma^2 + 4\kappa^2), \quad (54)$$

where $c^2 = 4\lambda^2(n - f - 1)^2 / (n - f)$.

For honest client h , the expectation of abnormal score $s_h^{(q)}$ from group q can be bounded as follows.

$$\mathbb{E}[s_h^{(q)}] = \mathbb{E}[\|\mathbf{g}_h^{(q)} - \hat{\mathbf{g}}^{(q)}\|] \quad (55)$$

$$\leq \mathbb{E}[\|\mathbf{g}_h^{(q)} - \bar{\mathbf{g}}_h^{(q)}\| + \|\bar{\mathbf{g}}_h^{(q)} - \bar{\mathbf{g}}^{(q)}\| + \|\bar{\mathbf{g}}^{(q)} - \mathbf{g}^{(q)}\| + \|\mathbf{g}^{(q)} - \hat{\mathbf{g}}^{(q)}\|] \quad (56)$$

$$= \mathbb{E}[\|\mathbf{g}_h^{(q)} - \bar{\mathbf{g}}_h^{(q)}\|] + \|\bar{\mathbf{g}}_h^{(q)} - \bar{\mathbf{g}}^{(q)}\| + \mathbb{E}[\|\bar{\mathbf{g}}^{(q)} - \mathbf{g}^{(q)}\|] + \mathbb{E}[\|\mathbf{g}^{(q)} - \hat{\mathbf{g}}^{(q)}\|] \quad (57)$$

$$\leq \sqrt{\mathbb{E}[\|\mathbf{g}_h^{(q)} - \bar{\mathbf{g}}_h^{(q)}\|^2]} + \|\bar{\mathbf{g}}_h^{(q)} - \bar{\mathbf{g}}^{(q)}\| + \sqrt{\mathbb{E}[\|\bar{\mathbf{g}}^{(q)} - \mathbf{g}^{(q)}\|^2]} + \sqrt{\mathbb{E}[\|\mathbf{g}^{(q)} - \hat{\mathbf{g}}^{(q)}\|^2]} \quad (58)$$

$$\leq (1 + \frac{1}{\sqrt{n-f}})\sigma + \kappa + c\sqrt{2\sigma^2 + 4\kappa^2}. \quad (59)$$

Here Inequality (56) is a result of triangular inequality, Inequality (58) comes from Cauchy inequality, and Inequality (59) is a combined result of Equation (54) and Sec. 6.

The variance of $s_h^{(q)}$ can be bounded as follows.

$$\text{Var}[s_h^{(q)}] = \mathbb{E}[(s_h^{(q)})^2] - (\mathbb{E}[s_h^{(q)}])^2 \quad (60)$$

$$\leq \mathbb{E}[(s_h^{(q)})^2] \quad (61)$$

$$= \mathbb{E}[\|\mathbf{g}_h^{(q)} - \hat{\mathbf{g}}^{(q)}\|^2] \quad (62)$$

$$= \mathbb{E}[\|(\mathbf{g}_h^{(q)} - \bar{\mathbf{g}}_h^{(q)}) + (\bar{\mathbf{g}}_h^{(q)} - \bar{\mathbf{g}}^{(q)}) + (\bar{\mathbf{g}}^{(q)} - \mathbf{g}^{(q)}) + (\mathbf{g}^{(q)} - \hat{\mathbf{g}}^{(q)})\|^2] \quad (63)$$

$$\leq 4\mathbb{E}[\|\mathbf{g}_h^{(q)} - \bar{\mathbf{g}}_h^{(q)}\|^2 + \|\bar{\mathbf{g}}_h^{(q)} - \bar{\mathbf{g}}^{(q)}\|^2 + \|\bar{\mathbf{g}}^{(q)} - \mathbf{g}^{(q)}\|^2 + \|\mathbf{g}^{(q)} - \hat{\mathbf{g}}^{(q)}\|^2]. \quad (64)$$

Here Inequality (64) is a result of Cauchy inequality.

We bound $\mathbb{E}[\|\bar{\mathbf{g}}^{(q)} - \mathbf{g}^{(q)}\|^2]$ as follows.

$$\mathbb{E}[\|\bar{\mathbf{g}}^{(q)} - \mathbf{g}^{(q)}\|^2] = \mathbb{E}[\|\frac{1}{n-f} \sum_{i \in \mathcal{H}} (\bar{\mathbf{g}}_i^{(q)} - \mathbf{g}_i^{(q)})\|^2] \quad (65)$$

$$= \frac{1}{(n-f)^2} \sum_{i \in \mathcal{H}} \mathbb{E}[\|\bar{\mathbf{g}}_i^{(q)} - \mathbf{g}_i^{(q)}\|^2] \quad (66)$$

$$\leq \frac{1}{(n-f)^2} \sum_{i \in \mathcal{H}} \sigma^2 \quad (67)$$

$$= \frac{\sigma^2}{n-f} \quad (68)$$

Here Equation (66) comes from the independence of minibatches sampling across different clients, and Inequality (67) is a result of Sec. 6.

Applying Sec. 6 and Equations (54) and (68) to Inequality (64), we have

$$\text{Var}[s_h^{(q)}] \leq 4(\sigma^2 + \kappa^2 + \frac{\sigma^2}{n-f} + c(2\sigma^2 + 4\kappa^2)) \quad (69)$$

$$= (4 + 8c^2 + \frac{4}{n-f})\sigma^2 + (4 + 16c^2)\kappa^2. \quad (70)$$

According to Inequality (59) and Equation (70), we can bound the expectation and variance of total abnormal score s_h of an honest client h .

$$\mathbb{E}[s_h] = \mathbb{E}\left[\sum_{q=1}^p s_h^{(q)}\right] \leq p(\sigma + \kappa + c\sqrt{2\sigma^2 + 4\kappa^2}) := A, \quad (71)$$

$$\text{Var}[s_h] = \sum_{q=1}^p \text{Var}[s_h^{(q)}] \leq p\left((4 + 8c^2 + \frac{4}{n-f})\sigma^2 + (4 + 16c^2)\kappa^2\right) := B. \quad (72)$$

Here the additive property of variance is a result of the independence of group abnormal scores $\{s_h^{(q)} \mid q \in [p]\}$, which comes from the independence of components in a gradient [36].

From Chebyshev's inequality, for any $\Delta_h > 0$ and honest client $h \in [n] \setminus \mathcal{B}$, we have

$$P(s_h < \mathbb{E}[s_h] + \Delta_h) \geq 1 - \frac{\text{Var}[s_h]}{\Delta_h^2}. \quad (73)$$

Consider the expectation of abnormal score $s_b^{(q)}$ from group q for Byzantine client $b \in \mathcal{B}$

$$\mathbb{E}[s_b^{(q)}] = \mathbb{E}[\|\mathbf{g}_b^{(q)} - \hat{\mathbf{g}}^{(q)}\|] \quad (74)$$

$$= \mathbb{E}[\|(\mathbf{g}_b^{(q)} - \bar{\mathbf{g}}^{(q)}) - (\hat{\mathbf{g}}^{(q)} - \bar{\mathbf{g}}^{(q)})\|] \quad (75)$$

$$\geq \mathbb{E}[\|\mathbf{g}_b^{(q)} - \bar{\mathbf{g}}^{(q)}\| - \|\hat{\mathbf{g}}^{(q)} - \bar{\mathbf{g}}^{(q)}\|] \quad (76)$$

$$\geq \mathbb{E}[\|\mathbf{g}_b^{(q)} - \bar{\mathbf{g}}^{(q)}\| - (\|\hat{\mathbf{g}}^{(q)} - \bar{\mathbf{g}}^{(q)}\| + \|\mathbf{g}^{(q)} - \bar{\mathbf{g}}^{(q)}\|)] \quad (77)$$

$$\geq \|\mathbf{g}_b^{(q)} - \bar{\mathbf{g}}^{(q)}\| - (\sqrt{\mathbb{E}[\|\hat{\mathbf{g}}^{(q)} - \bar{\mathbf{g}}^{(q)}\|^2]} + \sqrt{\mathbb{E}[\|\mathbf{g}^{(q)} - \bar{\mathbf{g}}^{(q)}\|^2]}) \quad (78)$$

$$\geq \delta_b - c\sqrt{2\sigma^2 + 4\kappa^2} - \frac{\sigma}{\sqrt{n-f}} \quad (79)$$

where $\delta_b = \|\mathbf{g}_b^{(q)} - \bar{\mathbf{g}}^{(q)}\|$ is the expected deviation of Byzantine client b from the average of honest gradients. Here the first and second inequalities come from triangular inequality, the third inequality is based on Cauchy inequality, and the 4-th inequality is a combined result of Equations (54) and (68).

The variance of abnormal score $s_b^{(q)}$ can be bounded as follows.

$$\text{Var}[s_b^{(q)}] = \text{Var}[\|\mathbf{g}_b^{(q)} - \hat{\mathbf{g}}^{(q)}\|] \quad (80)$$

$$\leq \mathbb{E}[\|(\mathbf{g}_b^{(q)} - \hat{\mathbf{g}}^{(q)}) - \mathbb{E}[\mathbf{g}_b^{(q)} - \hat{\mathbf{g}}^{(q)}]\|^2] \quad (81)$$

$$= \mathbb{E}[\|(\mathbf{g}_b^{(q)} - \mathbb{E}[\mathbf{g}_b^{(q)}]) - (\hat{\mathbf{g}}^{(q)} - \mathbb{E}[\hat{\mathbf{g}}^{(q)}])\|^2] \quad (82)$$

$$\leq 2\mathbb{E}[\|\mathbf{g}_b^{(q)} - \mathbb{E}[\mathbf{g}_b^{(q)}]\|^2 + \|\hat{\mathbf{g}}^{(q)} - \mathbb{E}[\hat{\mathbf{g}}^{(q)}]\|^2] \quad (83)$$

$$= 2\mathbb{E}\|\mathbf{g}_b^{(q)} - \mathbb{E}[\mathbf{g}_b^{(q)}]\|^2 + 2\mathbb{E}\|\hat{\mathbf{g}}^{(q)} - \mathbb{E}[\hat{\mathbf{g}}^{(q)}]\|^2 \quad (84)$$

The first inequality results from Lemma 2, and the second inequality comes from Cauchy inequality.

We bound $\|\hat{\mathbf{g}}^{(q)} - \mathbb{E}[\hat{\mathbf{g}}^{(q)}]\|$ as follows.

$$\mathbb{E}\|\hat{\mathbf{g}}^{(q)} - \mathbb{E}[\hat{\mathbf{g}}^{(q)}]\| = \mathbb{E}\|(\hat{\mathbf{g}}^{(q)} - \mathbf{g}^{(q)}) + (\mathbf{g}^{(q)} - \mathbb{E}[\mathbf{g}^{(q)}]) - \mathbb{E}[\hat{\mathbf{g}}^{(q)} - \mathbf{g}^{(q)}]\|^2 \quad (85)$$

$$\leq 3\mathbb{E}[\|\hat{\mathbf{g}}^{(q)} - \mathbf{g}^{(q)}\|^2 + \|\mathbf{g}^{(q)} - \mathbb{E}[\mathbf{g}^{(q)}]\|^2 + \|\mathbb{E}[\hat{\mathbf{g}}^{(q)} - \mathbf{g}^{(q)}]\|^2] \quad (86)$$

$$\leq 6\mathbb{E}\|\hat{\mathbf{g}}^{(q)} - \mathbf{g}^{(q)}\|^2 + 3\mathbb{E}\|\mathbf{g}^{(q)} - \mathbb{E}[\mathbf{g}^{(q)}]\|^2 \quad (87)$$

$$\leq 48(\sigma^2 + \kappa^2) + \frac{3\sigma^2}{n-f} \quad (88)$$

$$= (48 + \frac{3\sigma^2}{n-f})\sigma^2 + 48\kappa^2 \quad (89)$$

Apply Equation (89) to Equation (84), we have

$$\text{Var}[s_b^{(q)}] \leq 2\sigma_b^2 + (96 + \frac{6}{n-f})\sigma^2 + 96\kappa^2, \quad (90)$$

where $\sigma_b^2 = \mathbb{E}\|\mathbf{g}_b^{(q)} - \mathbb{E}\mathbf{g}_b^{(q)}\|^2$ is the variance.

Similar to Equations (71) and (72), we utilize Equations (79) and (90) to bound the expectation and variance of total abnormal score s_b of a byzantine client b .

$$\mathbb{E}[s_b] = \mathbb{E}\left[\sum_{q=1}^p s_b^{(q)}\right] \geq p(\delta_b 2\sqrt{2}c\sqrt{2\sigma^2 + 4\kappa^2} - \frac{\sigma}{\sqrt{n-f}}) := C, \quad (91)$$

$$\text{Var}[s_b] = \sum_{q=1}^p \text{Var}[s_b^{(q)}] \leq p(2\text{const} + (96 + \frac{6}{n-f})\sigma^2 + 96\kappa^2) := D \quad (92)$$

where $\delta_b = \mathbb{E}\|\mathbf{g}_b - \bar{\mathbf{g}}\|$. According to [17], σ_b^2 is bounded, i.e., $\sigma_b^2 \leq \text{const}$.

Similarly, we apply Chebyshev's inequality to the abnormal score of a Byzantine client $b \in \mathcal{B}$.

$$\Pr(s_b \geq \mathbb{E}[s_b] - \Delta_b) \geq 1 - \frac{\text{Var}[s_b]}{\Delta_b^2}, \quad b \in \mathcal{B}. \quad (93)$$

Combine Equations (71) to (73), and take $\Delta_h = (C - A)/(1 + \sqrt{D/B})$, we have

$$\Pr(s_h < \frac{\sqrt{D}A + \sqrt{B}C}{\sqrt{B} + \sqrt{D}}) = \Pr(s_h < A + \Delta_h) \quad (94)$$

$$\geq \Pr(s_h < \mathbb{E}[s_h] + \Delta_h) \quad (95)$$

$$\geq 1 - \frac{\text{Var}[s_h]}{\Delta_h^2} \quad (96)$$

$$\geq 1 - \frac{B}{\Delta_h^2} \quad (97)$$

$$= 1 - \frac{(\sqrt{B} + \sqrt{D})^2}{(C - A)^2}, \quad (98)$$

Combine Equations (91) to (93), and take $\Delta_b = (C - A)/(1 + \sqrt{B/D})$, we have

$$\Pr(s_b \geq \frac{\sqrt{D}A + \sqrt{B}C}{\sqrt{B} + \sqrt{D}}) \geq \Pr(s_b > C - \Delta_b) \quad (99)$$

$$\geq \Pr(s_b > \mathbb{E}[s_b] - \Delta) \quad (100)$$

$$\geq 1 - \frac{\text{Var}[s_b]}{\Delta^2} \quad (101)$$

$$\geq 1 - \frac{D}{\Delta_b^2}, \quad (102)$$

$$= 1 - \frac{(\sqrt{B} + \sqrt{D})^2}{(C - A)^2}, \quad (103)$$

Then consider the probability a Byzantine b is selected,

$$\Pr(b \in \tilde{\mathcal{B}}) = 1 - \Pr(b \notin \tilde{\mathcal{B}}) \quad (104)$$

$$\leq 1 - \Pr(s_h < \frac{\sqrt{D}A + \sqrt{B}C}{\sqrt{B} + \sqrt{D}}, \forall h \in \mathcal{H}, s_b > \frac{\sqrt{D}A + \sqrt{B}C}{\sqrt{B} + \sqrt{D}}) \quad (105)$$

$$= \Pr(s_h \geq \frac{\sqrt{D}A + \sqrt{B}C}{\sqrt{B} + \sqrt{D}}, \forall h \in \mathcal{H} \text{ or } s_b < \frac{\sqrt{D}A + \sqrt{B}C}{\sqrt{B} + \sqrt{D}}) \quad (106)$$

$$\leq \sum_{h \in \mathcal{H}} \Pr(s_h \geq \frac{\sqrt{D}A + \sqrt{B}C}{\sqrt{B} + \sqrt{D}}) + \Pr(s_b < \frac{\sqrt{D}A + \sqrt{B}C}{\sqrt{B} + \sqrt{D}}) \quad (107)$$

$$\leq (n - f + 1) \cdot \frac{(\sqrt{B} + \sqrt{D})^2}{(C - A)^2} \quad (108)$$

Solve $(n - f + 1) \cdot (\sqrt{B} + \sqrt{D})^2 / (C - A)^2 \leq \varepsilon$, we have

$$\begin{aligned} \mathbb{E}[\|\mathbf{g}_b - \bar{\mathbf{g}}\|] &\geq (1 + \frac{1}{\sqrt{n-f}})\sigma + \kappa + 2c\sqrt{2\sigma^2 + 4\kappa^2} \\ &\quad + \sqrt{\frac{n-f+1}{p\varepsilon}}(\sqrt{(4 + 16c^2 + \frac{4}{n-f})\sigma^2 + (4 + 8c^2)\kappa^2} \\ &\quad + \sqrt{2\text{const} + (96 + \frac{6}{n-f})\sigma^2 + 96\kappa^2}) \end{aligned} \quad (109)$$

which implies that the Byzantine gradients that deviate from the optimal gradient will be filtered by GAIN.

Therefore, for all $b \in \tilde{\mathcal{B}}$,

$$\mathbb{E}[\|\mathbf{g}_{\tilde{\mathcal{B}}} - \bar{\mathbf{g}}\|^2] \leq \mathcal{O}((\kappa^2 + \sigma^2)(1 + c^2 + \frac{1}{n-f})(1 + \frac{n-f+1}{p})) := C_1^2 \quad (110)$$

The elimination of ε is due to the sub-Gaussian property of $\mathbf{g}_{\tilde{\mathcal{B}}} - \bar{\mathbf{g}}$, which comes from the Gaussian property of benign gradients.

Combine Equations (48) and (110), $\mathbb{E}[\|\hat{\mathbf{g}} - \bar{\mathbf{g}}\|^2]$ is finally bounded as follows.

$$\mathbb{E}[\|\hat{\mathbf{g}} - \bar{\mathbf{g}}\|^2] \quad (111)$$

$$\leq \frac{|\tilde{\mathcal{H}}|^2}{(n-f)^2}(\sigma^2/\tilde{h} + \kappa^2) + \frac{|\tilde{\mathcal{B}}|^2}{(n-f)^2}C_1^2 \quad (112)$$

$$\leq \frac{(n-2f)^2}{(n-f)^2}(\sigma^2/(n-2f) + \kappa^2) + \frac{f^2}{(n-f)^2}C_1^2, \quad (113)$$

$$= \mathcal{O}((\kappa^2 + \sigma^2)(1 + \frac{n-f+1}{p})(1 + c^2 + \frac{1}{n-f})\frac{f^2}{(n-f)^2}) \quad (114)$$

which completes the proof. \square

B.1.1 Proof For The Main Proposition

Proof. According to the Lipschitz property of loss function \mathcal{L} , we have

$$\mathcal{L}(\mathbf{w}^t) - \mathcal{L}(\mathbf{w}^{t+1}) \geq \langle \nabla \mathcal{L}(\mathbf{w}^t), \mathbf{w}^t - \mathbf{w}^{t+1} \rangle - \frac{L}{2} \|\mathbf{w}^t - \mathbf{w}^{t+1}\|^2. \quad (115)$$

Since $\mathbf{w}^t - \mathbf{w}^{t+1} = \nabla \mathcal{L}(\mathbf{w}^t) + (\hat{\mathbf{g}}^t - \nabla \mathcal{L}(\mathbf{w}^t))$, we can write Equation (115) as follows

$$\begin{aligned} \mathcal{L}(\mathbf{w}^t) - \mathcal{L}(\mathbf{w}^{t+1}) &\geq (\eta - \frac{L}{2}\eta^2) \|\nabla \mathcal{L}(\mathbf{w}^t)\|^2 \\ &\quad + (\eta - \frac{L}{2}\eta^2) \langle \nabla \mathcal{L}(\mathbf{w}^t), \hat{\mathbf{g}}^t - \nabla \mathcal{L}(\mathbf{w}^t) \rangle \\ &\quad - \frac{L}{2}\eta^2 \|\hat{\mathbf{g}}^t - \nabla \mathcal{L}(\mathbf{w}^t)\|^2. \end{aligned} \quad (116)$$

Then, we bound inner product term $\langle \nabla \mathcal{L}(\mathbf{w}^t), \hat{\mathbf{g}}^t - \nabla \mathcal{L}(\mathbf{w}^t) \rangle$.

$$|\langle \nabla \mathcal{L}(\mathbf{w}^t), \hat{\mathbf{g}}^t - \nabla \mathcal{L}(\mathbf{w}^t) \rangle| \leq \|\nabla \mathcal{L}(\mathbf{w}^t)\| \cdot \|\hat{\mathbf{g}}^t - \nabla \mathcal{L}(\mathbf{w}^t)\| \quad (117)$$

$$\leq \frac{1}{2} \|\nabla \mathcal{L}(\mathbf{w}^t)\|^2 + 2 \|\hat{\mathbf{g}}^t - \nabla \mathcal{L}(\mathbf{w}^t)\|^2 \quad (118)$$

Combine Equations (116) and (118) and we have

$$\begin{aligned} \mathcal{L}(\mathbf{w}^t) - \mathcal{L}(\mathbf{w}^{t+1}) &\geq (\eta - \frac{L}{2}\eta^2) \|\nabla \mathcal{L}(\mathbf{w}^t)\|^2 \\ &\quad + (\eta - \frac{L}{2}\eta^2) \cdot -(\frac{1}{2} \|\nabla \mathcal{L}(\mathbf{w}^t)\|^2 + 2 \|\hat{\mathbf{g}}^t - \nabla \mathcal{L}(\mathbf{w}^t)\|^2) \\ &\quad - \frac{L}{2}\eta^2 \|\hat{\mathbf{g}}^t - \nabla \mathcal{L}(\mathbf{w}^t)\|^2 \end{aligned} \quad (119)$$

$$= (\frac{1}{2}\eta - \frac{L}{4}\eta^2) \|\nabla \mathcal{L}(\mathbf{w}^t)\|^2 - (2\eta - \frac{L}{2}\eta^2) \|\hat{\mathbf{g}}^t - \nabla \mathcal{L}(\mathbf{w}^t)\|^2 \quad (120)$$

Take the expectation on both sides of Equation (120), we have

$$\mathbb{E}[\mathcal{L}(\mathbf{w}^t) - \mathcal{L}(\mathbf{w}^{t+1})] \geq (\frac{1}{2}\eta - \frac{L}{4}\eta^2)\mathbb{E}[\|\nabla\mathcal{L}(\mathbf{w}^t)\|^2] - (2\eta - \frac{L}{2}\eta^2)\mathbb{E}[\|\hat{\mathbf{g}}^t - \nabla\mathcal{L}(\mathbf{w}^t)\|^2]. \quad (121)$$

Apply Lemma 3 to Inequality (121) and sum over $t = 0, 1, \dots, T - 1$, then we have

$$\mathbb{E}[\mathcal{L}(\mathbf{w}^0) - \mathcal{L}(\mathbf{w}^T)] \geq (\frac{1}{2}\eta - \frac{L}{4}\eta^2) \sum_{t=1}^T \mathbb{E}[\|\nabla\mathcal{L}(\mathbf{w}^t)\|^2] - T(\frac{1}{2}\eta - \frac{L}{2}\eta^2)C^2. \quad (122)$$

where $C^2 = \mathcal{O}((\kappa^2 + \sigma^2)(1 + (n - f + 1)/p)(1 + c^2 + 1/(n - f))\frac{f^2}{(n - f)^2})$

Take $\eta = 1/2L$, and consider that the loss function is generally non-negative, e.g., cross-entropy loss, ℓ_2 loss,

$$\mathbb{E}[\mathcal{L}(\mathbf{w}^0)] \geq \frac{3}{16L} \sum_{t=1}^T (\mathbb{E}[\|\nabla\mathcal{L}(\mathbf{w}^t)\|^2] - \frac{2}{3}C^2), \quad (123)$$

which completes the proof. \square

B.2 Comparison of Our Convergence Results with Recent Works

Recent works [13, 19, 25] also analyze the convergence of Byzantine-robust FL in the non-IID setting. We compare our convergence results with them.

Similarity. We all provided convergence guarantees of the same type, i.e., we all guarantee that we can reach an approximate optimal point after a certain number of communication rounds. Moreover, we all admit that convergence in presence of Byzantine clients may be impossible due to non-IID data, i.e., $\|\nabla\mathcal{L}(\mathbf{w})\|$ may never decrease to zero.

Differences. The convergence analysis comes from different aspects of defending against the Byzantine attack. In particular, [25] consider the impact of the aggregation rules; [13] focus on bucketing together with momentum; [37] consider a combined effect of client variance reduction and aggregation rules; and we concentrate more on gradient dimensions. From this perspective, our result is orthogonal to previous ones.

More detailed differences are as follows: [25] focus on decentralized FL with a server and provide an order optimal upper bound. However, this strong result requires a Byzantine ratio lower than $1/3$. By contrast, we consider a centralized FL setting and only assume the Byzantine ratio to be lower than $1/2$. [37] consider an ideal case where the objective function is strongly convex, while we consider a more general non-convex case.

C Experiment Setup

C.1 Setup for Main Experiments in Section 7

Data distribution. For CIFAR-10, CIFAR-100 [26] and ImageNet-12, we use Dirichlet distribution to generate non-IID data by following [38, 39]. In particular, for each client i , we sample $p_i^y \sim \text{Dir}(\beta)$ and allocate a p_i^y proportion of the data of label y to client i , where $\text{Dir}(\beta)$ represents the Dirichlet distribution with a concentration parameter β . We follow [39] and set the number of clients $n = 50$ and the concentration parameter $\beta = 0.5$ as default.

Other setups. The setups for datasets FEMNIST [30], CIFAR-10 [26], CIFAR-100 [26] and ImageNet-12 [29] are listed in below Table 4.

Table 4: Default experimental settings for FEMNIST, CIFAR-10, CIFAR-100 and ImageNet-12.

Dataset	FEMNIST	CIFAR-10	CIFAR-100	ImageNet-12
Architecture	CNN [30] ResNet-18 [34]	AlexNet [33]	SqueezeNet	
# Communication rounds	1000	200	400	200
Client sample ratio	0.005	0.1	0.1	0.1
# Local epochs	1	5	1	1
Optimizer	SGD	SGD	SGD	SGD
Batch size	64	64	64	128
Learning rate	0.5	0.1	0.1	0.1
Momentum	0.5	0.5	0.5	0.9
Weight decay	0.0001	0.0001	0.0001	0.0001
Learning rate decay	No	No	No	Reduce to 0.01 after 100-th communication round
Gradient clipping	Yes	Yes	Yes	Yes
Clipping norm	2	2	2	2

Three types of attacks based on the adversary’s knowledge are considered:

- Agnostic attack: the adversary knows neither honest gradients nor the AGR.
- Partial knowledge attack: the adversary only has the knowledge of honest gradients.
- Omniscient attack: the adversary knows both honest gradients and the AGR.

Among the six attacks considered: BitFlip [19], LabelFlip [19] are agnostic attacks; LIE [31], Min-Max [17], Min-Sum [17] are partial knowledge attacks; and IPM [32] is an omniscient attack.

The hyperparameters of six attacks: BitFlip [19], LabelFlip [19], LIE [31], Min-Max [17], Min-Sum [17], IPM [32], are listed in below Table 5.

Table 5: The hyperparameters of six attacks.

Attacks	Hyperparameters
BitFlip	N/A
LabelFlip	N/A
LIE	$z = 1.5$
Min-Max	$\gamma_{\text{init}} = 10, \tau = 1 \times 10^{-5}, \delta$: coordinate-wise standard deviation
Min-Sum	$\gamma_{\text{init}} = 10, \tau = 1 \times 10^{-5}, \delta$: coordinate-wise standard deviation
IPM	# eval = 2

The hyperparameters of six defenses: Multi-Krum [4], Bulyan [5], Median [8], RFA [18], DnC [17], RBTM [25], are listed in below Table 5.

C.2 Setup for Experiments on the Number of Sub-vectors in Section 7

The number of client is set to $n = 50$. The samples are partitioned in a Dirichlet manner with concentration parameter $\beta = 0.5$. Please refer to Sec. 7.1 for the details of Dirichlet partition. The number of Byzantine clients is set to $f = 10$. LIE [31] attack with $z = 1.5$ considered.

Table 6: The default hyperparameters of the AGRs.

AGRs	Hyperparameters
Multi-Krum	N/A
Bulyan	N/A
Median	N/A
RFA	$T = 3$
DnC	$c = 4, \text{niters} = 1, b = 10000$
RBTM	N/A

We use AlexNet [33] as the model architecture. The number of communication rounds is set to 500. In each communication round, all client participate in the training.

For local training, the number of local epochs is set to 1, batch size is set to 64, the optimizer is set to SGD. For SGD optimizer, learning rate is set to 0.1, momentum is set to 0.5, weight decay coefficient is set to 0.0001. We also adopt gradient clipping with clipping norm 2.

Two defenses are considered: a radical AGR Multi-Krum [4] and a conservative AGR Bulyan [5].

D GAIN mitigates the deviation of aggregated gradients

In Sec. 6, we claim that our GAIN method can reduce the deviation of aggregated gradient \hat{g} from the average of honest gradients g . To verify this fact, we compare the deviation of the aggregated gradient of different defenses and their GAIN variants in Figure 3. In particular, we use $\|\hat{g} - g\|$, the distance between the aggregated gradient \hat{g} and the average of honest gradients g to measure the deviation degree. As shown in Figure 3, the gradient deviation degree of GAIN-enhanced defenses is much lower than their original versions as expected, which validates that our GAIN can mitigate the gradient deviation.

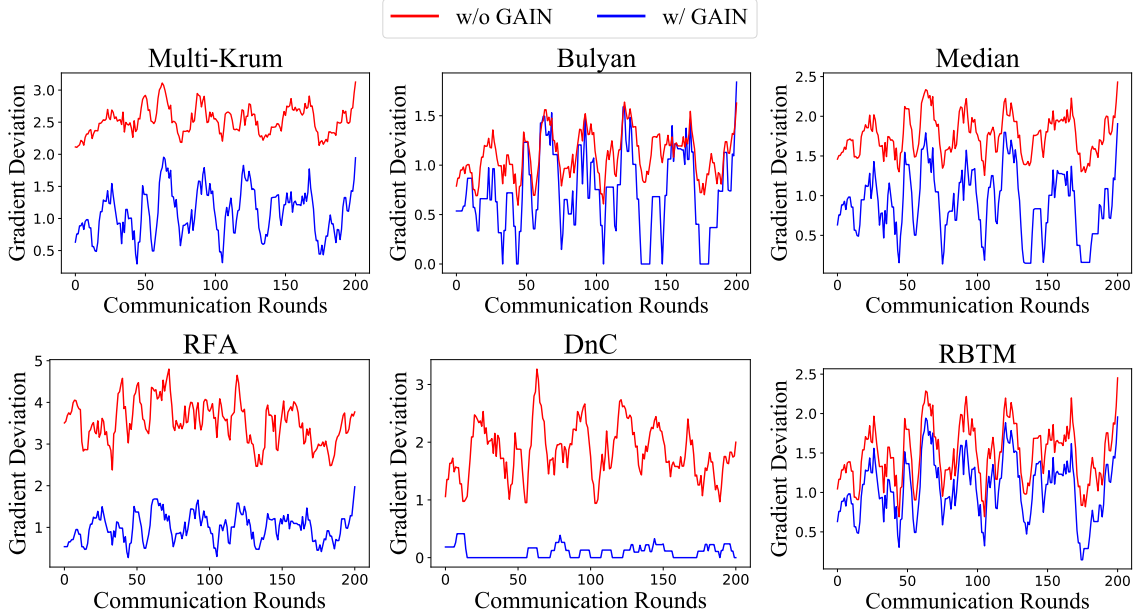


Figure 3: The gradient deviation $\|\hat{g} - g\|$ of six different defenses w/ and w/o GAIN under LIE attack on CIFAR-10. The lower the better.

E Results on different number of clients.

We also conduct experiments across different number of clients. Table 7 demonstrates the results of different defenses under LIE attack across $n = \{75, 100\}$ clients on CIFAR-10 dataset. Note that the number of Byzantine clients is set to $f = 0.2 \cdot n$ correspondingly. Other setups follow the default setup of the main experiments in Sec. 3 and Appendix C. As evidenced by Table 7, integrating current robust AGRs into our GAIN outperforms their original versions across all client numbers.

Table 7: Accuracy (mean \pm std) of different defenses against LIE attack under different client numbers on CIFAR-10.

n	Multi-Krum	Multi-Krum+GAIN	Bulyan	Bulyan+GAIN	Median	Median+GAIN
75	28.72 \pm 0.71	54.89 \pm 0.16	23.37 \pm 1.22	51.11 \pm 0.00	44.89 \pm 2.98	52.22 \pm 1.64
100	32.49 \pm 1.22	56.51 \pm 0.01	21.93 \pm 0.55	46.49 \pm 1.33	33.82 \pm 0.21	46.12 \pm 0.17
n	RFA	RFA+GAIN	DnC	DnC+GAIN	RBTM	RBTM+GAIN
75	16.89 \pm 1.38	49.85 \pm 0.06	59.31 \pm 1.33	59.75 \pm 0.42	45.06 \pm 0.96	50.24 \pm 0.31
100	14.01 \pm 1.34	49.85 \pm 1.97	58.88 \pm 1.45	59.61 \pm 1.19	40.38 \pm 0.48	47.02 \pm 0.03